

# Topics on String Phenomenology\*

I. Antoniadis<sup>†</sup>

Department of Physics, CERN - Theory Division,  
1211 Geneva 23, Switzerland

October 25, 2018

These lectures present some topics of string phenomenology and contain two parts.

In the first part, I review the possibility of lowering the string scale in the TeV region, that provides a theoretical framework for solving the mass hierarchy problem and unifying all interactions. The apparent weakness of gravity can then be accounted by the existence of large internal dimensions, in the sub-millimeter region, and transverse to a braneworld where our universe must be confined. I review the main properties of this scenario and its implications for observations at both particle colliders, and in non-accelerator gravity experiments.

In the second part, I discuss a simple framework of toroidal string models with magnetized branes, that offers an interesting self-consistent setup for string phenomenology. I will present an algorithm for fixing the geometric parameters of the compactification, build calculable particle physics models such as a supersymmetric  $SU(5)$  Grand Unified Theory with three generations of quarks and leptons, and implement low energy supersymmetry breaking with gauge mediation that can be studied directly at the string level.

---

\*Lectures given at Les Houches 2007 Summer School 'String Theory and the Real World - From particle physics to astrophysics', 2 - 27 July 2007

<sup>†</sup>On leave from CPHT (UMR CNRS 7644) Ecole Polytechnique, F-91128 Palaiseau

# Contents

<b>1</b>	<b>Introduction</b>	<b>3</b>
<b>2</b>	<b>Framework of low scale strings</b>	<b>5</b>
<b>3</b>	<b>Experimental implications in accelerators</b>	<b>6</b>
3.1	World-brane extra dimensions . . . . .	6
3.2	Extra large transverse dimensions . . . . .	9
3.3	String effects . . . . .	10
<b>4</b>	<b>Supersymmetry in the bulk and short range forces</b>	<b>11</b>
4.1	Sub-millimeter forces . . . . .	11
4.2	Brane non-linear supersymmetry . . . . .	12
<b>5</b>	<b>Electroweak symmetry breaking</b>	<b>14</b>
<b>6</b>	<b>Standard Model on D-branes</b>	<b>18</b>
6.1	Hypercharge embedding and the weak angle . . . . .	19
6.2	The fate of $U(1)$ 's, proton stability and neutrino masses . . . . .	21
<b>7</b>	<b>Internal magnetic fields</b>	<b>22</b>
<b>8</b>	<b>Minimal Standard Model embedding</b>	<b>23</b>
<b>9</b>	<b>Moduli stabilization</b>	<b>25</b>
9.1	Supersymmetry conditions . . . . .	27
9.2	Tadpole cancellation conditions . . . . .	30
9.3	Spectrum . . . . .	32
9.4	A supersymmetric $SU(5)$ GUT with stabilized moduli . . . . .	33
<b>10</b>	<b>Gaugino masses and D-term gauge mediation</b>	<b>34</b>

# 1 Introduction

During the last few decades, physics beyond the Standard Model (SM) was guided from the problem of mass hierarchy. This can be formulated as the question of why gravity appears to us so weak compared to the other three known fundamental interactions corresponding to the electromagnetic, weak and strong nuclear forces. Indeed, gravitational interactions are suppressed by a very high energy scale, the Planck mass  $M_P \sim 10^{19}$  GeV, associated to a length  $l_P \sim 10^{-35}$  m, where they are expected to become important. In a quantum theory, the hierarchy implies a severe fine tuning of the fundamental parameters in more than 30 decimal places in order to keep the masses of elementary particles at their observed values. The reason is that quantum radiative corrections to all masses generated by the Higgs vacuum expectation value (VEV) are proportional to the ultraviolet cutoff which in the presence of gravity is fixed by the Planck mass. As a result, all masses are “attracted” to become about  $10^{16}$  times heavier than their observed values.

Besides compositeness, there are three main ideas that have been proposed and studied extensively during the last years, corresponding to different approaches of dealing with the mass hierarchy problem. (1) Low energy supersymmetry with all superparticle masses in the TeV region. Indeed, in the limit of exact supersymmetry, quadratically divergent corrections to the Higgs self-energy are exactly cancelled, while in the softly broken case, they are cutoff by the supersymmetry breaking mass splittings. (2) TeV scale strings, in which quadratic divergences are cutoff by the string scale and low energy supersymmetry is not needed. (3) Split supersymmetry, where scalar masses are heavy while fermions (gauginos and higgsinos) are light. Thus, gauge coupling unification and dark matter candidate are preserved but the mass hierarchy should be stabilized by a different way and the low energy world appears to be fine-tuned. All these ideas are experimentally testable at high-energy particle colliders and in particular at LHC. Below, I discuss their implementation in string theory.

The appropriate and most convenient framework for low energy supersymmetry and grand unification is the perturbative heterotic string. Indeed, in this theory, gravity and gauge interactions have the same origin, as massless modes of the closed heterotic string, and they are unified at the string scale  $M_s$ . As a result, the Planck mass  $M_P$  is predicted to be proportional to  $M_s$ :

$$M_P = M_s/g, \tag{1}$$

where  $g$  is the gauge coupling. In the simplest constructions all gauge couplings are the same at the string scale, given by the four-dimensional (4d) string coupling, and thus no grand unified group is needed for unification. In our conventions  $\alpha_{\text{GUT}} = g^2 \simeq 0.04$ , leading to a discrepancy between the string and grand unification scale  $M_{\text{GUT}}$  by almost two orders of magnitude. Explaining this gap introduces in general new parameters or a new scale, and the predictive power is essentially lost. This is the main defect of this framework, which remains though an open and interesting possibility [1].

The other two ideas have both as natural framework of realization type I string theory with D-branes. Unlike in the heterotic string, gauge and gravitational interactions have now different origin. The latter are described again by closed strings, while the former emerge as excitations of open strings with endpoints confined on D-branes [2]. This leads to a braneworld description of our universe, which should be localized on a hypersurface, i.e. a membrane extended in  $p$  spatial dimensions, called  $p$ -brane (see Fig. 1). Closed strings propagate in all nine dimensions of string theory: in those extended along the  $p$ -brane, called parallel, as well as in the transverse ones. On the contrary, open strings are attached on the  $p$ -brane. Obviously, our  $p$ -brane world must have

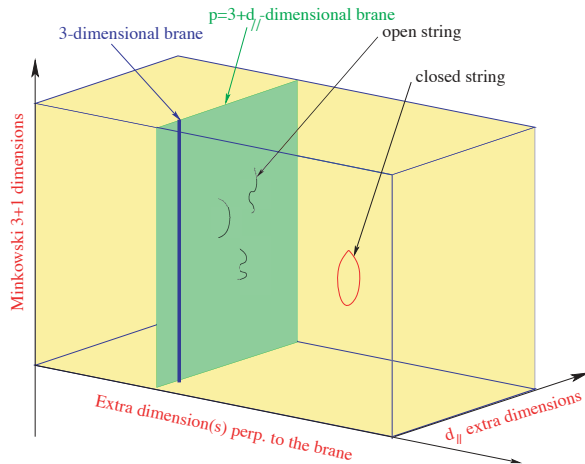


Figure 1: In the type I string framework, our Universe contains, besides the three known spatial dimensions (denoted by a single blue line), some extra dimensions ( $d_{||} = p - 3$ ) parallel to our world  $p$ -brane (green plane) where endpoints of open strings are confined, as well as some transverse dimensions (yellow space) where only gravity described by closed strings can propagate.

at least the three known dimensions of space. But it may contain more: the extra  $d_{||} = p - 3$  parallel dimensions must have a finite size, in order to be unobservable at present energies, and can be as large as  $\text{TeV}^{-1} \sim 10^{-18} \text{ m}$  [3]. On the other hand, transverse dimensions interact with us only gravitationally and experimental bounds are much weaker: their size should be less than about 0.1 mm [4]. In the following, I review the main properties and experimental signatures of low string scale models [5, 6].

These lectures have two parts. In the first part, contained in sections 2 to 6, I describe the implementation, the properties and the main physical properties of low scale string theories. In the second part, contained in the following sections, starting from section 7, I discuss a simple framework of toroidal type I string compactifications with in general high string scale, in the presence of

magnetized branes, that can be used for moduli stabilization, model building and supersymmetry breaking.

## 2 Framework of low scale strings

In type I theory, the different origin of gauge and gravitational interactions implies that the relation between the Planck and string scales is not linear as (1) of the heterotic string. The requirement that string theory should be weakly coupled, constrain the size of all parallel dimensions to be of order of the string length, while transverse dimensions remain unrestricted. Assuming an isotropic transverse space of  $n = 9 - p$  compact dimensions of common radius  $R_\perp$ , one finds:

$$M_P^2 = \frac{1}{g_s^4} M_s^{2+n} R_\perp^n, \quad g_s \simeq g^2. \quad (2)$$

where  $g_s$  is the string coupling. It follows that the type I string scale can be chosen hierarchically smaller than the Planck mass [5, 7] at the expense of introducing extra large transverse dimensions felt only by gravity, while keeping the string coupling small [5]. The weakness of 4d gravity compared to gauge interactions (ratio  $M_W/M_P$ ) is then attributed to the largeness of the transverse space  $R_\perp$  compared to the string length  $l_s = M_s^{-1}$ .

An important property of these models is that gravity becomes effectively  $(4+n)$ -dimensional with a strength comparable to those of gauge interactions at the string scale. The first relation of Eq. (2) can be understood as a consequence of the  $(4+n)$ -dimensional Gauss law for gravity, with

$$M_*^{(4+n)} = M_s^{2+n}/g^4 \quad (3)$$

the effective scale of gravity in  $4+n$  dimensions. Taking  $M_s \simeq 1$  TeV, one finds a size for the extra dimensions  $R_\perp$  varying from  $10^8$  km, .1 mm, down to a Fermi for  $n = 1, 2$ , or 6 large dimensions, respectively. This shows that while  $n = 1$  is excluded,  $n \geq 2$  is allowed by present experimental bounds on gravitational forces [4, 8]. Thus, in these models, gravity appears to us very weak at macroscopic scales because its intensity is spread in the “hidden” extra dimensions. At distances shorter than  $R_\perp$ , it should deviate from Newton’s law, which may be possible to explore in laboratory experiments (see Fig. 2).

The main experimental implications of TeV scale strings in particle accelerators are of three types, in correspondence with the three different sectors that are generally present: (i) new compactified parallel dimensions, (ii) new extra large transverse dimensions and low scale quantum gravity, and (iii) genuine string and quantum gravity effects. On the other hand, there exist interesting implications in non accelerator table-top experiments due to the exchange of gravitons or other possible states living in the bulk.

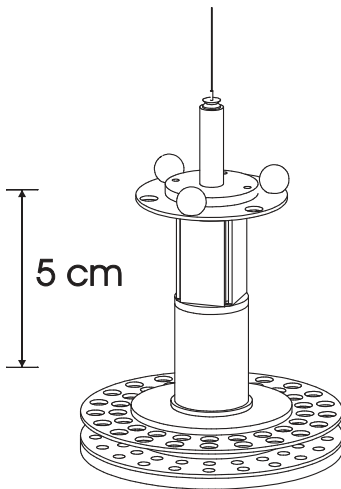


Figure 2: Torsion pendulum that tested Newton’s law at  $55 \mu\text{m}$ .

### 3 Experimental implications in accelerators

#### 3.1 World-brane extra dimensions

In this case  $RM_s \gtrsim 1$ , and the associated compactification scale  $R_{\parallel}^{-1}$  would be the first scale of new physics that should be found increasing the beam energy [3, 9, 10]. There are several reasons for the existence of such dimensions. It is a logical possibility, since out of the six extra dimensions of string theory only two are needed for lowering the string scale, and thus the effective  $p$ -brane of our world has in general  $d_{\parallel} \equiv p - 3 \leq 4$ . Moreover, they can be used to address several physical problems in braneworld models, such as obtaining different SM gauge couplings, explaining fermion mass hierarchies due to different localization points of quarks and leptons in the extra dimensions, providing calculable mechanisms of supersymmetry breaking, etc.

The main consequence is the existence of Kaluza-Klein (KK) excitations for all SM particles that propagate along the extra parallel dimensions. Their masses are given by:

$$M_m^2 = M_0^2 + \frac{m^2}{R_{\parallel}^2} \quad ; \quad m = 0, \pm 1, \pm 2, \dots \quad (4)$$

where we used  $d_{\parallel} = 1$ , and  $M_0$  is the higher dimensional mass. The zero-mode  $m = 0$  is identified with the 4d state, while the higher modes have the same quantum numbers with the lowest one, except for their mass given in (4). There are two types of experimental signatures of such dimensions [9, 11, 12]: (i) virtual exchange of KK excitations, leading to deviations in cross-sections compared to

the SM prediction, that can be used to extract bounds on the compactification scale; (ii) direct production of KK modes.

On general grounds, there can be two different kinds of models with qualitatively different signatures depending on the localization properties of matter fermion fields. If the latter are localized in 3d brane intersections, they do not have excitations and KK momentum is not conserved because of the breaking of translation invariance in the extra dimension(s). KK modes of gauge bosons are then singly produced giving rise to generally strong bounds on the compactification scale and new resonances that can be observed in experiments. Otherwise, they can be produced only in pairs due to the KK momentum conservation, making the bounds weaker but the resonances difficult to observe.

When the internal momentum is conserved, the interaction vertex involving KK modes has the same 4d tree-level gauge coupling. On the other hand, their couplings to localized matter have an exponential form factor suppressing the interactions of heavy modes. This form factor can be viewed as the fact that the branes intersection has a finite thickness. For instance, the coupling of the KK excitations of gauge fields  $A^\mu(x, y) = \sum_m A_m^\mu \exp i \frac{my}{R_\parallel}$  to the charge density  $j_\mu(x)$  of massless localized fermions is described by the effective action [13]:

$$\int d^4x \sum_m e^{-\ln 16 \frac{m^2 l_s^2}{2R_\parallel^2}} j_\mu(x) A_m^\mu(x). \quad (5)$$

After Fourier transform in position space, it becomes:

$$\int d^4x dy \frac{1}{(2\pi \ln 16)^2} e^{-\frac{y^2 M_s^2}{2 \ln 16}} j_\mu(x) A^\mu(x, y), \quad (6)$$

from which we see that localized fermions form a Gaussian distribution of charge with a width  $\sigma = \sqrt{\ln 16} l_s \sim 1.66 l_s$ .

To simplify the analysis, let us consider first the case  $d_\parallel = 1$  where some of the gauge fields arise from an effective 4-brane, while fermions are localized states on brane intersections. Since the corresponding gauge couplings are reduced by the size of the large dimension  $R_\parallel M_s$  compared to the others, one can account for the ratio of the weak to strong interactions strengths if the  $SU(2)$  brane extends along the extra dimension, while  $SU(3)$  does not. As a result, there are 3 distinct cases to study [12], denoted by  $(t, l, l)$ ,  $(t, l, t)$  and  $(t, t, l)$ , where the three positions in the brackets correspond to the three SM gauge group factors  $SU(3) \times SU(2) \times U(1)$  and those with  $l$  (longitudinal) feel the extra dimension, while those with  $t$  (transverse) do not.

In the  $(t, l, l)$  case, there are KK excitations of  $SU(2) \times U(1)$  gauge bosons:  $W_\pm^{(m)}$ ,  $\gamma^{(m)}$  and  $Z^{(m)}$ . Performing a  $\chi^2$  fit of the electroweak observables, one finds that if the Higgs is a bulk state ( $l$ ),  $R_\parallel^{-1} \gtrsim 3.5$  TeV [14]. This implies that LHC can produce at most the first KK mode. Different choices for localization of matter and Higgs fields lead to bounds, lying in the range 1 – 5 TeV [14].

In addition to virtual effects, KK excitations can be produced on-shell at LHC as new resonances [11] (see Fig. 3). There are two different channels,

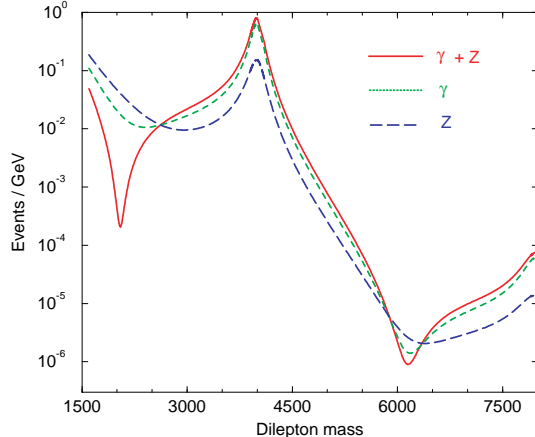


Figure 3: Production of the first KK modes of the photon and of the  $Z$  boson at LHC, decaying to electron-positron pairs. The number of expected events is plotted as a function of the energy of the pair in GeV. From highest to lowest: excitation of  $\gamma + Z$ ,  $\gamma$  and  $Z$ .

neutral Drell–Yan processes  $pp \rightarrow l^+l^-X$  and the charged channel  $l^\pm\nu$ , corresponding to the production of the KK modes  $\gamma^{(1)}$ ,  $Z^{(1)}$  and  $W_\pm^{(1)}$ , respectively. The discovery limits are about 6 TeV, while the exclusion bounds 15 TeV. An interesting observation in the case of  $\gamma^{(1)} + Z^{(1)}$  is that interferences can lead to a “dip” just before the resonance. There are some ways to distinguish the corresponding signals from other possible origin of new physics, such as models with new gauge bosons. In fact, in the  $(t, l, l)$  and  $(t, l, t)$  cases, one expects two resonances located practically at the same mass value. This property is not shared by most of other new gauge boson models. Moreover, the heights and widths of the resonances are directly related to those of SM gauge bosons in the corresponding channels.

In the  $(t, l, t)$  case, only the  $SU(2)$  factor feels the extra dimension and the limits set by the KK states of  $W^\pm$  remain the same. On the other hand, in the  $(t, t, l)$  case where only  $U(1)_Y$  feels the extra dimension, the limits are weaker and the exclusion bound is around 8 TeV. In addition to these simple possibilities, brane constructions lead often to cases where part of  $U(1)_Y$  is  $t$  and part is  $l$ . If  $SU(2)$  is  $l$  the limits come again from  $W^\pm$ , while if it is  $t$  then it will be difficult to distinguish this case from a generic extra  $U(1)'$ . A good statistics would be needed to see the deviation in the tail of the resonance as being due to effects additional to those of a generic  $U(1)'$  resonance. Finally, in the case of two or more parallel dimensions, the sum in the exchange of the KK modes diverges in the limit  $R_\parallel M_s \gg 1$  and needs to be regularized using the form factor (5). Cross-sections become bigger yielding stronger bounds, while

Table 1: Limits on  $R_{\perp}$  in mm.

Experiment	$n = 2$	$n = 4$	$n = 6$
Collider bounds			
LEP 2	$5 \times 10^{-1}$	$2 \times 10^{-8}$	$7 \times 10^{-11}$
Tevatron	$5 \times 10^{-1}$	$10^{-8}$	$4 \times 10^{-11}$
LHC	$4 \times 10^{-3}$	$6 \times 10^{-10}$	$3 \times 10^{-12}$
NLC	$10^{-2}$	$10^{-9}$	$6 \times 10^{-12}$
Present non-collider bounds			
SN1987A	$3 \times 10^{-4}$	$10^{-8}$	$6 \times 10^{-10}$
COMPTEL	$5 \times 10^{-5}$	-	-

resonances are closer implying that more of them could be reached by LHC.

On the other hand, if all SM particles propagate in the extra dimension (called universal)<sup>1</sup>, KK modes can only be produced in pairs and the lower bound on the compactification scale becomes weaker, of order of 300-500 GeV. Moreover, no resonances can be observed at LHC, so that this scenario appears very similar to low energy supersymmetry. In fact, KK parity can even play the role of R-parity, implying that the lightest KK mode is stable and can be a dark matter candidate in analogy to the LSP [15].

### 3.2 Extra large transverse dimensions

The main experimental signal is gravitational radiation in the bulk from any physical process on the world-brane. In fact, the very existence of branes breaks translation invariance in the transverse dimensions and gravitons can be emitted from the brane into the bulk. During a collision of center of mass energy  $\sqrt{s}$ , there are  $\sim (\sqrt{s}R_{\perp})^n$  KK excitations of gravitons with tiny masses, that can be emitted. Each of these states looks from the 4d point of view as a massive, quasi-stable, extremely weakly coupled ( $s/M_P^2$  suppressed) particle that escapes from the detector. The total effect is a missing-energy cross-section roughly of order:

$$\frac{(\sqrt{s}R_{\perp})^n}{M_P^2} \sim \frac{1}{s} \left( \frac{\sqrt{s}}{M_s} \right)^{n+2}. \quad (7)$$

Explicit computation of these effects leads to the bounds given in Table 1. However, larger radii are allowed if one relaxes the assumption of isotropy, by taking for instance two large dimensions with different radii.

Fig. 4 shows the cross-section for graviton emission in the bulk, corresponding to the process  $pp \rightarrow jet + graviton$  at LHC, together with the SM background [16]. For a given value of  $M_s$ , the cross-section for graviton emission decreases with the number of large transverse dimensions, in contrast to the

---

<sup>1</sup>Although interesting, this scenario seems difficult to be realized, since 4d chirality requires non-trivial action of orbifold twists with localized chiral states at the fixed points.

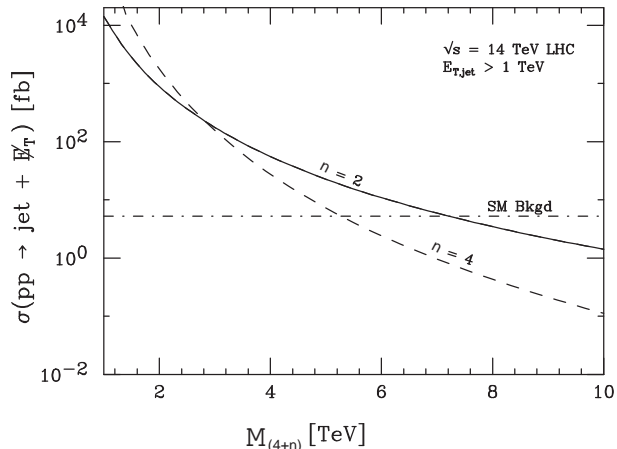


Figure 4: Missing energy due to graviton emission at LHC, as a function of the higher-dimensional gravity scale  $M_*$ , produced together with a hadronic jet. The expected cross-section is shown for  $n = 2$  and  $n = 4$  extra dimensions, together with the SM background.

case of parallel dimensions. The reason is that gravity becomes weaker if there are more dimensions because there is more space for the gravitational field to escape. There is a particular energy and angular distribution of the produced gravitons that arise from the distribution in mass of KK states of spin-2. This can be contrasted to other sources of missing energy and might be a smoking gun for the extra dimensional nature of such a signal.

In Table 1, there are also included astrophysical and cosmological bounds. Astrophysical bounds [17, 18] arise from the requirement that the radiation of gravitons should not carry on too much of the gravitational binding energy released during core collapse of supernovae. In fact, the measurements of Kamiokande and IMB for SN1987A suggest that the main channel is neutrino fluxes. The best cosmological bound [19] is obtained from requiring that decay of bulk gravitons to photons do not generate a spike in the energy spectrum of the photon background measured by the COMPTEL instrument. Bulk gravitons are expected to be produced just before nucleosynthesis due to thermal radiation from the brane. The limits assume that the temperature was at most 1 MeV as nucleosynthesis begins, and become stronger if temperature is increased.

### 3.3 String effects

At low energies, the interaction of light (string) states is described by an effective field theory. Their exchange generates in particular four-fermion operators that can be used to extract independent bounds on the string scale. In analogy

with the bounds on longitudinal extra dimensions, there are two cases depending on the localization properties of matter fermions. If they come from open strings with both ends on the same stack of branes, exchange of massive open string modes gives rise to dimension eight effective operators, involving four fermions and two space-time derivatives [13, 20]. The corresponding bounds on the string scale are then around 500 GeV. On the other hand, if matter fermions are localized on non-trivial brane intersections, one obtains dimension six four-fermion operators and the bounds become stronger:  $M_s \gtrsim 2 - 3$  TeV [6, 13]. At energies higher than the string scale, new spectacular phenomena are expected to occur, related to string physics and quantum gravity effects, such as possible micro-black hole production [21–23]. Particle accelerators would then become the best tools for studying quantum gravity and string theory.

## 4 Supersymmetry in the bulk and short range forces

### 4.1 Sub-millimeter forces

Besides the spectacular predictions in accelerators, there are also modifications of gravitation in the sub-millimeter range, which can be tested in “table-top” experiments that measure gravity at short distances. There are three categories of such predictions:

(i) Deviations from the Newton’s law  $1/r^2$  behavior to  $1/r^{2+n}$ , which can be observable for  $n = 2$  large transverse dimensions of sub-millimeter size. This case is particularly attractive on theoretical grounds because of the logarithmic sensitivity of SM couplings on the size of transverse space [24], that allows to determine the hierarchy [25].

(ii) New scalar forces in the sub-millimeter range, related to the mechanism of supersymmetry breaking, and mediated by light scalar fields  $\varphi$  with masses [5, 26]:

$$m_\varphi \simeq \frac{m_{susy}^2}{M_P} \simeq 10^{-4} - 10^{-6} \text{ eV}, \quad (8)$$

for a supersymmetry breaking scale  $m_{susy} \simeq 1 - 10$  TeV. They correspond to Compton wavelengths of 1 mm to 10  $\mu\text{m}$ .  $m_{susy}$  can be either  $1/R_{\parallel}$  if supersymmetry is broken by compactification [26], or the string scale if it is broken “maximally” on our world-brane [5]. A universal attractive scalar force is mediated by the radion modulus  $\varphi \equiv M_P \ln R$ , with  $R$  the radius of the longitudinal or transverse dimension(s). In the former case, the result (8) follows from the behavior of the vacuum energy density  $\Lambda \sim 1/R_{\parallel}^4$  for large  $R_{\parallel}$  (up to logarithmic corrections). In the latter, supersymmetry is broken primarily on the brane, and thus its transmission to the bulk is gravitationally suppressed, leading to (8). For  $n = 2$ , there may be an enhancement factor of the radion mass by  $\ln R_{\perp} M_s \simeq 30$  decreasing its wavelength by an order of magnitude [25].

The coupling of the radius modulus to matter relative to gravity can be

easily computed and is given by:

$$\sqrt{\alpha_\varphi} = \frac{1}{M} \frac{\partial M}{\partial \varphi}; \quad \alpha_\varphi = \begin{cases} \frac{\partial \ln \Lambda_{\text{QCD}}}{\partial \ln R} \simeq \frac{1}{3} & \text{for } R_{\parallel} \\ \frac{2n}{n+2} = 1 - 1.5 & \text{for } R_{\perp} \end{cases} \quad (9)$$

where  $M$  denotes a generic physical mass. In the longitudinal case, the coupling arises dominantly through the radius dependence of the QCD gauge coupling [26], while in the case of transverse dimension, it can be deduced from the rescaling of the metric which changes the string to the Einstein frame and depends slightly on the bulk dimensionality ( $\alpha = 1 - 1.5$  for  $n = 2 - 6$ ) [25]. Such a force can be tested in microgravity experiments and should be contrasted with the change of Newton's law due the presence of extra dimensions that is observable only for  $n = 2$  [4, 8]. The resulting bounds from an analysis of the radion effects are [27]:

$$M_* \gtrsim 6 \text{ TeV}. \quad (10)$$

In principle there can be other light moduli which couple with even larger strengths. For example the dilaton, whose VEV determines the string coupling, if it does not acquire large mass from some dynamical supersymmetric mechanism, can lead to a force of strength 2000 times bigger than gravity [28]. (iii) Non universal repulsive forces much stronger than gravity, mediated by possible abelian gauge fields in the bulk [17, 29]. Such fields acquire tiny masses of the order of  $M_s^2/M_P$ , as in (8), due to brane localized anomalies [29]. Although their gauge coupling is infinitesimally small,  $g_A \sim M_s/M_P \simeq 10^{-16}$ , it is still bigger than the gravitational coupling  $E/M_P$  for typical energies  $E \sim 1 \text{ GeV}$ , and the strength of the new force would be  $10^6 - 10^8$  stronger than gravity. This is an interesting region which will be soon explored in micro-gravity experiments (see Fig. 5). Note that in this case supernova constraints impose that there should be at least four large extra dimensions in the bulk [17].

In Fig. 5 we depict the actual information from previous, present and upcoming experiments [8, 25]. The solid lines indicate the present limits from the experiments indicated. The excluded regions lie above these solid lines. Measuring gravitational strength forces at short distances is challenging. The horizontal lines correspond to theoretical predictions, in particular for the graviton in the case  $n = 2$  and for the radion in the transverse case. These limits are compared to those obtained from particle accelerator experiments in Table 1. Finally, in Figs. 6 and 7, we display recent improved bounds for new forces at very short distances by focusing on the left hand side of Fig. 5, near the origin [8].

## 4.2 Brane non-linear supersymmetry

When the closed string sector is supersymmetric, supersymmetry on a generic brane configuration is non-linearly realized even if the spectrum is not supersymmetric and brane fields have no superpartners. The reason is that the gravitino must couple to a conserved current locally, implying the existence of a goldstino on the brane world-volume [30]. The goldstino is exactly massless in the infinite

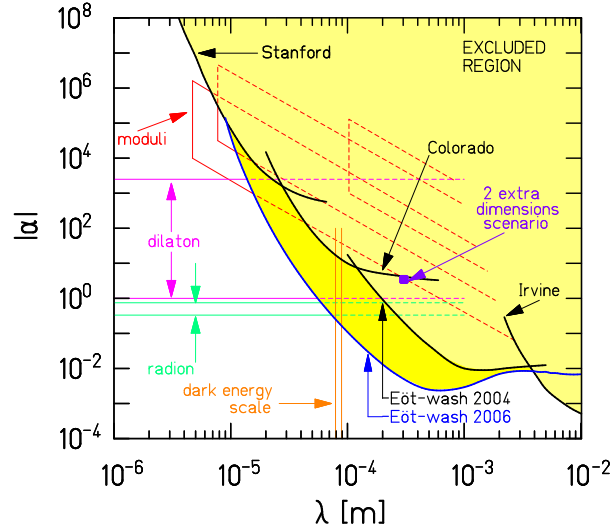


Figure 5: Present limits on new short-range forces (yellow regions), as a function of their range  $\lambda$  and their strength relative to gravity  $\alpha$ . The limits are compared to new forces mediated by the graviton in the case of two large extra dimensions, and by the radion.

(transverse) volume limit and is expected to acquire a small mass suppressed by the volume, of order (8). In the standard realization, its coupling to matter is given via the energy momentum tensor [31], while in general there are more terms invariant under non-linear supersymmetry that have been classified, up to dimension eight [32, 33].

An explicit computation was performed for a generic intersection of two brane stacks, leading to three irreducible couplings, besides the standard one [33]: two of dimension six involving the goldstino, a matter fermion and a scalar or gauge field, and one four-fermion operator of dimension eight. Their strength is set by the goldstino decay constant  $\kappa$ , up to model-independent numerical coefficients which are independent of the brane angles. Obviously, at low energies the dominant operators are those of dimension six. In the minimal case of (non-supersymmetric) SM, only one of these two operators may exist, that couples the goldstino  $\chi$  with the Higgs  $H$  and a lepton doublet  $L$ :

$$\mathcal{L}_\chi^{int} = 2\kappa(D_\mu H)(LD^\mu \chi) + h.c., \quad (11)$$

where the goldstino decay constant is given by the total brane tension

$$\frac{1}{2\kappa^2} = N_1 T_1 + N_2 T_2; \quad T_i = \frac{M_s^4}{4\pi^2 g_i^2}, \quad (12)$$

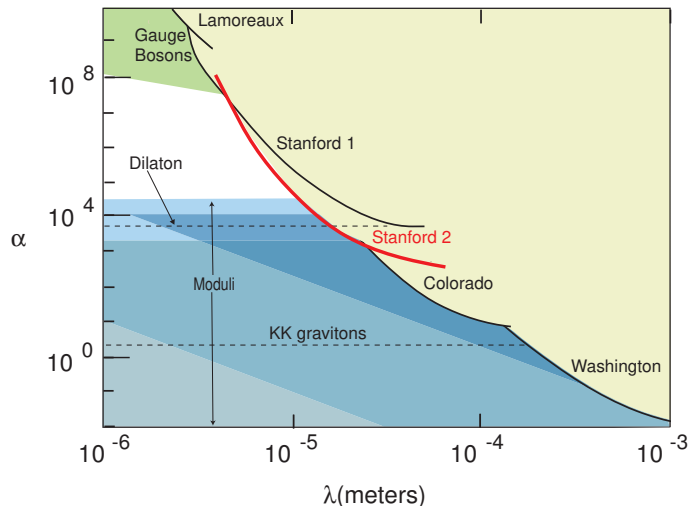


Figure 6: Bounds on non-Newtonian forces in the range 6-20  $\mu\text{m}$  (see S. J. Smullin et al. [8]).

with  $N_i$  the number of branes in each stack. It is important to notice that the effective interaction (11) conserves the total lepton number  $L$ , as long as we assign to the goldstino a total lepton number  $L(\chi) = -1$  [34]. To simplify the analysis, we will consider the simplest case where (11) exists only for the first generation and  $L$  is the electron doublet [34].

The effective interaction (11) gives rise mainly to the decays  $W^\pm \rightarrow e^\pm \chi$  and  $Z, H \rightarrow \nu \chi$ . It turns out that the invisible  $Z$  width gives the strongest limit on  $\kappa$  which can be translated to a bound on the string scale  $M_s \gtrsim 500$  GeV, comparable to other collider bounds. This allows for the striking possibility of a Higgs boson decaying dominantly, or at least with a sizable branching ratio, via such an invisible mode, for a wide range of the parameter space  $(M_s, m_H)$ , as seen in Fig. 8.

## 5 Electroweak symmetry breaking

Non-supersymmetric TeV strings offer also a framework to realize gauge symmetry breaking radiatively. Indeed, from the effective field theory point of view, one expects quadratically divergent one-loop contributions to the masses of scalar fields. The divergences are cut off by  $M_s$  and if the corrections are negative, they can induce electroweak symmetry breaking and explain the mild hierarchy between the weak and a string scale at a few TeV, in terms of a loop factor [35]. More precisely, in the minimal case of one Higgs doublet  $H$ , the scalar potential is:

$$V = \lambda(H^\dagger H)^2 + \mu^2(H^\dagger H), \quad (13)$$

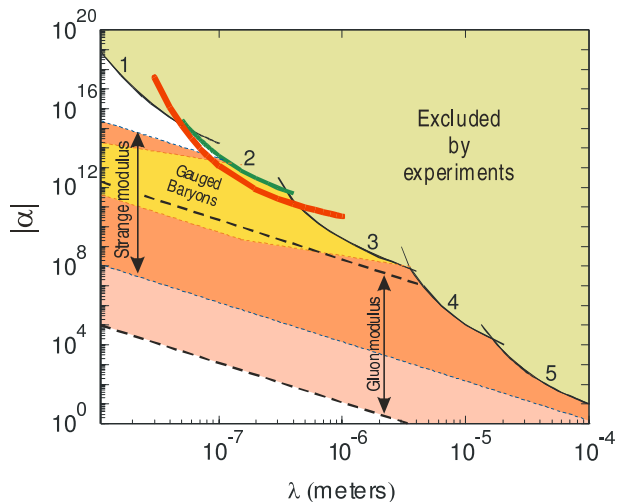


Figure 7: Bounds on non-Newtonian forces in the range of 10-200 nm (see R. S. Decca et al. in Ref. [8]). Curves 4 and 5 correspond to Stanford and Colorado experiments, respectively, of Fig. 6 (see also J C. Long and J. C. Price of Ref. [8]).

where  $\lambda$  arises at tree-level. Moreover, in any model where the Higgs field comes from an open string with both ends fixed on the same brane stack, it is given by an appropriate truncation of a supersymmetric theory. Within the minimal spectrum of the SM,  $\lambda = (g_2^2 + g'^2)/8$ , with  $g_2$  and  $g'$  the  $SU(2)$  and  $U(1)_Y$  gauge couplings. On the other hand,  $\mu^2$  is generated at one loop:

$$\mu^2 = -\varepsilon^2 g^2 M_s^2, \quad (14)$$

where  $\varepsilon$  is a loop factor that can be estimated from a toy model computation and varies in the region  $\varepsilon \sim 10^{-1} - 10^{-3}$ .

Indeed, consider for illustration a simple case where the whole one-loop effective potential of a scalar field can be computed. We assume for instance one extra dimension compactified on a circle of radius  $R > 1$  (in string units). An interesting situation is provided by a class of models where a non-vanishing VEV for a scalar (Higgs) field  $\phi$  results in shifting the mass of each KK excitation by a constant  $a(\phi)$ :

$$M_m^2 = \left( \frac{m + a(\phi)}{R} \right)^2, \quad (15)$$

with  $m$  the KK integer momentum number. Such mass shifts arise for instance in the presence of a Wilson line,  $a = q \oint \frac{dy}{2\pi} g A$ , where  $A$  is the internal component of a gauge field with gauge coupling  $g$ , and  $q$  is the charge of a given state under the corresponding generator. A straightforward computation shows that the

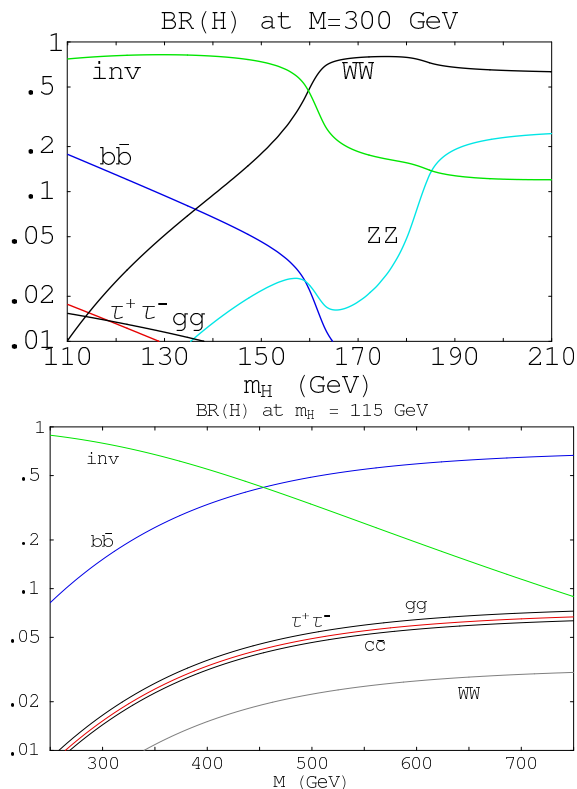


Figure 8: Higgs branching ratios, as functions either of the Higgs mass  $m_H$  for a fixed value of the string scale  $M_s \simeq 2M = 600$  GeV, or of  $M \simeq M_s/2$  for  $m_H = 115$  GeV.

$\phi$ -dependent part of the one-loop effective potential is given by [36]:

$$V_{eff} = -Tr(-)^F \frac{R}{32\pi^{3/2}} \sum_n e^{2\pi i n a} \int_0^\infty dl l^{3/2} f_s(l) e^{-\pi^2 n^2 R^2 l} \quad (16)$$

where  $F = 0, 1$  for bosons and fermions, respectively. We have included a regulating function  $f_s(l)$  which contains for example the effects of string oscillators. To understand its role we will consider the two limits  $R \gg 1$  and  $R \ll 1$ . In the first case only the  $l \rightarrow 0$  region contributes to the integral. This means that the effective potential receives sizable contributions only from the infrared (field theory) degrees of freedom. In this limit we would have  $f_s(l) \rightarrow 1$ . For example, in the string model considered in [35]:

$$f_s(l) = \left[ \frac{1}{4l} \frac{\theta_2}{\eta^3} \left( il + \frac{1}{2} \right) \right]^4 \rightarrow 1 \quad \text{for } l \rightarrow 0, \quad (17)$$

and the field theory result is finite and can be explicitly computed. As a result

of the Taylor expansion around  $a = 0$ , we are able to extract the one-loop contribution to the coefficient of the term of the potential quadratic in the Higgs field. It is given by a loop factor times the compactification scale [36]. One thus obtains  $\mu^2 \sim g^2/R^2$  up to a proportionality constant which is calculable in the effective field theory. On the other hand, if we consider  $R \rightarrow 0$ , which by  $T$ -duality corresponds to taking the extra dimension as transverse and very large, the one-loop effective potential receives contributions from the whole tower of string oscillators as appearing in  $f_s(l)$ , leading to squared masses given by a loop factor times  $M_s^2$ , according to eq. (14).

More precisely, from the expression (16), one finds:

$$\varepsilon^2(R) = \frac{1}{2\pi^2} \int_0^\infty \frac{dl}{(2l)^{5/2}} \frac{\theta_2^4}{4\eta^{12}} \left( il + \frac{1}{2} \right) R^3 \sum_n n^2 e^{-2\pi n^2 R^2 l}, \quad (18)$$

which is plotted in Fig. 9. For the asymptotic value  $R \rightarrow 0$  (corresponding upon

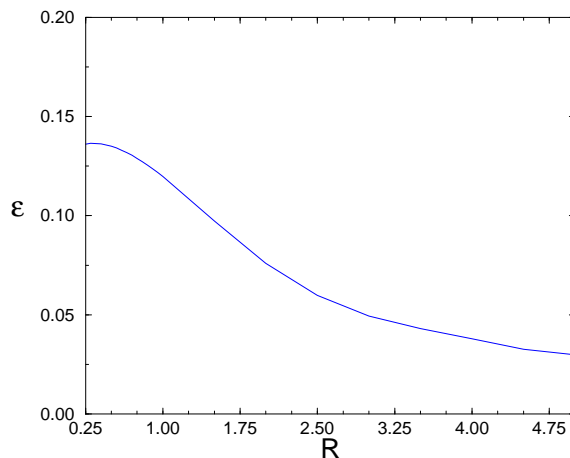


Figure 9: The coefficient  $\varepsilon$  of the one loop Higgs mass (14).

$T$ -duality to a large transverse dimension of radius  $1/R$ ),  $\varepsilon(0) \simeq 0.14$ , and the effective cut-off for the mass term is  $M_s$ , as can be seen from Eq. (14). At large  $R$ ,  $\mu^2(R)$  falls off as  $1/R^2$ , which is the effective cut-off in the limit  $R \rightarrow \infty$ , as we argued above, in agreement with field theory results in the presence of a compactified extra dimension [26, 37]. In fact, in the limit  $R \rightarrow \infty$ , an analytic approximation to  $\varepsilon(R)$  gives:

$$\varepsilon(R) \simeq \frac{\varepsilon_\infty}{M_s R}, \quad \varepsilon_\infty^2 = \frac{3\zeta(5)}{4\pi^4} \simeq 0.008. \quad (19)$$

The potential (13) has the usual minimum, given by the VEV of the neutral component of the Higgs doublet  $v = \sqrt{-\mu^2/\lambda}$ . Using the relation of  $v$  with the

$Z$  gauge boson mass,  $M_Z^2 = (g_2^2 + g'^2)v^2/4$ , and the expression of the quartic coupling  $\lambda$ , one obtains for the Higgs mass a prediction which is the Minimal Supersymmetric Standard Model (MSSM) value for  $\tan\beta \rightarrow \infty$  and  $m_A \rightarrow \infty$ :  $m_H = M_Z$ . The tree level Higgs mass is known to receive important radiative corrections from the top-quark sector and rises to values around 120 GeV. Furthermore, from (14), one can compute  $M_s$  in terms of the Higgs mass  $m_H^2 = -2\mu^2$ :

$$M_s = \frac{m_H}{\sqrt{2}g\varepsilon}, \quad (20)$$

yielding naturally values in the TeV range.

## 6 Standard Model on D-branes

The gauge group closest to the Standard Model one can easily obtain with D-branes is  $U(3) \times U(2) \times U(1)$ . The first factor arises from three coincident ‘‘color’’ D-branes. An open string with one end on them is a triplet under  $SU(3)$  and carries the same  $U(1)$  charge for all three components. Thus, the  $U(1)$  factor of  $U(3)$  has to be identified with *gauged* baryon number. Similarly,  $U(2)$  arises from two coincident ‘‘weak’’ D-branes and the corresponding abelian factor is identified with *gauged* weak-doublet number. Finally, an extra  $U(1)$  D-brane is necessary in order to accommodate the Standard Model without breaking the baryon number [38]. In principle this  $U(1)$  brane can be chosen to be independent of the other two collections with its own gauge coupling. To improve the predictability of the model, we choose to put it on top of either the color or the weak D-branes [39]. In either case, the model has two independent gauge couplings  $g_3$  and  $g_2$  corresponding, respectively, to the gauge groups  $U(3)$  and  $U(2)$ . The  $U(1)$  gauge coupling  $g_1$  is equal to either  $g_3$  or  $g_2$ .

Let us denote by  $Q_3$ ,  $Q_2$  and  $Q_1$  the three  $U(1)$  charges of  $U(3) \times U(2) \times U(1)$ , in a self explanatory notation. Under  $SU(3) \times SU(2) \times U(1)_3 \times U(1)_2 \times U(1)_1$ , the members of a family of quarks and leptons have the following quantum numbers:

$$\begin{aligned} Q & (\mathbf{3}, \mathbf{2}; 1, w, 0)_{1/6} \\ u^c & (\bar{\mathbf{3}}, \mathbf{1}; -1, 0, x)_{-2/3} \\ d^c & (\bar{\mathbf{3}}, \mathbf{1}; -1, 0, y)_{1/3} \\ L & (\mathbf{1}, \mathbf{2}; 0, 1, z)_{-1/2} \\ l^c & (\mathbf{1}, \mathbf{1}; 0, 0, 1)_1 \end{aligned} \quad (21)$$

The values of the  $U(1)$  charges  $x, y, z, w$  will be fixed below so that they lead to the right hypercharges, shown for completeness as subscripts.

It turns out that there are two possible ways of embedding the Standard Model particle spectrum on these stacks of branes [38], which are shown pictorially in Fig. 10. The quark doublet  $Q$  corresponds necessarily to a massless excitation of an open string with its two ends on the two different collections

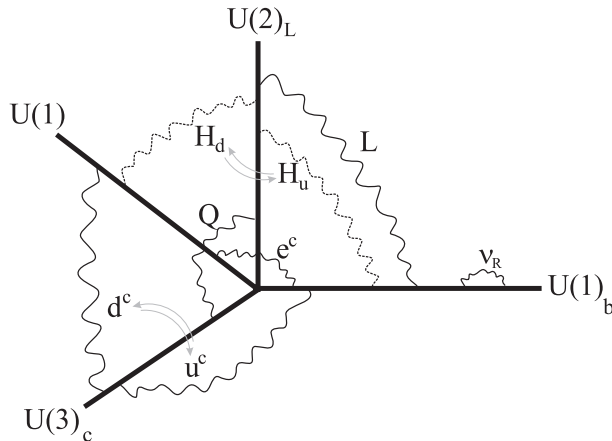


Figure 10: A minimal Standard Model embedding on D-branes.

of branes (color and weak). As seen from the figure, a fourth brane stack is needed for a complete embedding, which is chosen to be a  $U(1)_b$  extended in the bulk. This is welcome since one can accommodate right handed neutrinos as open string states on the bulk with sufficiently small Yukawa couplings suppressed by the large volume of the bulk [40]. The two models are obtained by an exchange of the up and down antiquarks,  $u^c$  and  $d^c$ , which correspond to open strings with one end on the color branes and the other either on the  $U(1)$  brane, or on the  $U(1)_b$  in the bulk. The lepton doublet  $L$  arises from an open string stretched between the weak branes and  $U(1)_b$ , while the antilepton  $l^c$  corresponds to a string with one end on the  $U(1)$  brane and the other in the bulk. For completeness, we also show the two possible Higgs states  $H_u$  and  $H_d$  that are both necessary in order to give tree-level masses to all quarks and leptons of the heaviest generation.

### 6.1 Hypercharge embedding and the weak angle

The weak hypercharge  $Y$  is a linear combination of the three  $U(1)$ 's:

$$Y = Q_1 + \frac{1}{2}Q_2 + c_3Q_3 \quad ; \quad c_3 = -1/3 \text{ or } 2/3, \quad (22)$$

where  $Q_N$  denotes the  $U(1)$  generator of  $U(N)$  normalized so that the fundamental representation of  $SU(N)$  has unit charge. The corresponding  $U(1)$  charges appearing in eq. (21) are  $x = -1$  or  $0$ ,  $y = 0$  or  $1$ ,  $z = -1$ , and  $w = 1$  or  $-1$ , for  $c_3 = -1/3$  or  $2/3$ , respectively. The hypercharge coupling  $g_Y$  is given

by <sup>2</sup>:

$$\frac{1}{g_Y^2} = \frac{2}{g_1^2} + \frac{4c_2^2}{g_2^2} + \frac{6c_3^2}{g_3^2}. \quad (23)$$

It follows that the weak angle  $\sin^2 \theta_W$ , is given by:

$$\sin^2 \theta_W \equiv \frac{g_Y^2}{g_2^2 + g_Y^2} = \frac{1}{2 + 2g_2^2/g_1^2 + 6c_3^2 g_2^2/g_3^2}, \quad (24)$$

where  $g_N$  is the gauge coupling of  $SU(N)$  and  $g_1 = g_2$  or  $g_1 = g_3$  at the string scale. In order to compare the theoretical predictions with the experimental value of  $\sin^2 \theta_W$  at  $M_s$ , we plot in Fig. 11 the corresponding curves as functions of  $M_s$ . The solid line is the experimental curve. The dashed line is the plot

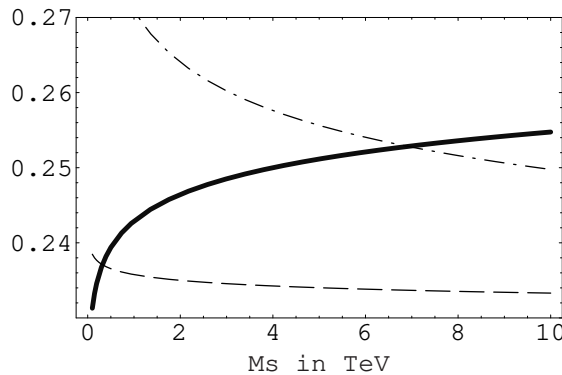


Figure 11: The experimental value of  $\sin^2 \theta_W$  (thick curve), and the theoretical predictions (24).

of the function (24) for  $g_1 = g_2$  with  $c_3 = -1/3$  while the dotted-dashed line corresponds to  $g_1 = g_3$  with  $c_3 = 2/3$ . The other two possibilities are not shown because they lead to a value of  $M_s$  which is too high to protect the hierarchy. Thus, the second case, where the  $U(1)$  brane is on top of the color branes, is compatible with low energy data for  $M_s \sim 6 - 8$  TeV and  $g_s \simeq 0.9$ .

From Eq. (24) and Fig. 11, we find the ratio of the  $SU(2)$  and  $SU(3)$  gauge couplings at the string scale to be  $\alpha_2/\alpha_3 \sim 0.4$ . This ratio can be arranged by an appropriate choice of the relevant moduli. For instance, one may choose the color and  $U(1)$  branes to be D3 branes while the weak branes to be D7 branes. Then, the ratio of couplings above can be explained by choosing the volume of the four compact dimensions of the seven branes to be  $V_4 = 2.5$  in string units. This being larger than one is consistent with the picture above. Moreover it

<sup>2</sup>The gauge couplings  $g_{2,3}$  are determined at the tree-level by the string coupling and other moduli, like radii of longitudinal dimensions. In higher orders, they also receive string threshold corrections.

predicts an interesting spectrum of KK states for the Standard model, different from the naive choices that have appeared hitherto: the only Standard Model particles that have KK descendants are the W bosons as well as the hypercharge gauge boson. However, since the hypercharge is a linear combination of the three  $U(1)$ 's, the massive  $U(1)$  KK gauge bosons do not couple to the hypercharge but to the weak doublet number.

## 6.2 The fate of $U(1)$ 's, proton stability and neutrino masses

It is easy to see that the remaining three  $U(1)$  combinations orthogonal to  $Y$  are anomalous. In particular there are mixed anomalies with the  $SU(2)$  and  $SU(3)$  gauge groups of the Standard Model. These anomalies are cancelled by three axions coming from the closed string RR (Ramond) sector, via the standard Green-Schwarz mechanism [41]. The mixed anomalies with the non-anomalous hypercharge are also cancelled by dimension five Chern-Simmons type of interactions [38]. An important property of the above Green-Schwarz anomaly cancellation mechanism is that the anomalous  $U(1)$  gauge bosons acquire masses leaving behind the corresponding global symmetries. This is in contrast to what would had happened in the case of an ordinary Higgs mechanism. These global symmetries remain exact to all orders in type I string perturbation theory around the orientifold vacuum. This follows from the topological nature of Chan-Paton charges in all string amplitudes. On the other hand, one expects non-perturbative violation of global symmetries and consequently exponentially small in the string coupling, as long as the vacuum stays at the orientifold point. Thus, all  $U(1)$  charges are conserved and since  $Q_3$  is the baryon number, proton stability is guaranteed.

Another linear combination of the  $U(1)$ 's is the lepton number. Lepton number conservation is important for the extra dimensional neutrino mass suppression mechanism described above, that can be destabilized by the presence of a large Majorana neutrino mass term. Such a term can be generated by the lepton-number violating dimension five effective operator  $LLHH$  that leads, in the case of TeV string scale models, to a Majorana mass of the order of a few GeV. Even if we manage to eliminate this operator in some particular model, higher order operators would also give unacceptably large contributions, as we focus on models in which the ratio between the Higgs vacuum expectation value and the string scale is just of order  $\mathcal{O}(1/10)$ . The best way to protect tiny neutrino masses from such contributions is to impose lepton number conservation.

A bulk neutrino propagating in  $4 + n$  dimensions can be decomposed in a series of 4d KK excitations denoted collectively by  $\{m\}$ :

$$S_{kin} = R_{\perp}^n \int d^4x \sum_{\{m\}} \left\{ \bar{\nu}_{Rm} \not{\partial} \nu_{Rm} + \bar{\nu}_{Rm}^c \not{\partial} \nu_{Rm}^c + \frac{m}{R_{\perp}} \nu_{Rm} \nu_{Rm}^c + c.c. \right\}, \quad (25)$$

where  $\nu_R$  and  $\nu_R^c$  are the two Weyl components of the Dirac spinor and for simplicity we considered a common compactification radius  $R_{\perp}$ . On the other hand, there is a localized interaction of  $\nu_R$  with the Higgs field and the lepton

doublet, which leads to mass terms between the left-handed neutrino and the KK states  $\nu_{Rm}$ , upon the Higgs VEV  $v$ :

$$S_{int} = g_s \int d^4x H(x) L(x) \nu_R(x, y=0) \quad \rightarrow \quad \frac{g_s v}{R_\perp^{n/2}} \sum_m \nu_L \nu_{Rm}, \quad (26)$$

in strings units. Since the mass mixing  $g_s v / R_\perp^{n/2}$  is much smaller than the KK mass  $1/R_\perp$ , it can be neglected for all the excitations except for the zero-mode  $\nu_{R0}$ , which gets a Dirac mass with the left-handed neutrino

$$m_\nu \simeq \frac{g_s v}{R_\perp^{n/2}} \simeq v \frac{M_s}{M_p} \simeq 10^{-3} - 10^{-2} \text{ eV}, \quad (27)$$

for  $M_s \simeq 1 - 10$  TeV, where the relation (2) was used. In principle, with one bulk neutrino, one could try to explain both solar and atmospheric neutrino oscillations using also its first KK excitation. However, the later behaves like a sterile neutrino which is now excluded experimentally. Therefore, one has to introduce three bulk species (at least two)  $\nu_R^i$  in order to explain neutrino oscillations in a ‘traditional way’, using their zero-modes  $\nu_{R0}^i$  [42]. The main difference with the usual seesaw mechanism is the Dirac nature of neutrino masses, which remains an open possibility to be tested experimentally.

## 7 Internal magnetic fields

We now consider type I string theory, or equivalently type IIB with orientifold 9-planes and D9-branes [2]. Upon compactification in four dimensions on a Calabi-Yau manifold, one gets  $\mathcal{N} = 2$  supersymmetry in the bulk and  $\mathcal{N} = 1$  on the branes. We then turn on internal magnetic fields [43, 44], which, in the T-dual picture, amounts to intersecting branes [45, 46]. For generic angles, or equivalently for arbitrary magnetic fields, supersymmetry is spontaneously broken and described by effective D-terms in the four-dimensional (4d) theory [43]. In the weak field limit,  $|H|\alpha' < 1$  with  $\alpha'$  the string Regge slope, the resulting mass shifts are given by:

$$\delta M^2 = (2k + 1)|qH| + 2qH\Sigma \quad ; \quad k = 0, 1, 2, \dots, \quad (28)$$

where  $H$  is the magnetic field of an abelian gauge symmetry, corresponding to a Cartan generator of the higher dimensional gauge group, on a non-contractible 2-cycle of the internal manifold.  $\Sigma$  is the corresponding projection of the spin operator,  $k$  is the Landau level and  $q = q_L + q_R$  is the charge of the state, given by the sum of the left and right charges of the endpoints of the associated open string. We recall that the exact string mass formula has the same form as (28) with  $qH$  replaced by:

$$qH \longrightarrow \theta_L + \theta_R \quad ; \quad \theta_{L,R} = \arctan(q_{L,R} H \alpha'). \quad (29)$$

Obviously, the field theory expression (28) is reproduced in the weak field limit.

The Gauss law for the magnetic flux implies that the field  $H$  is quantized in terms of the area of the corresponding 2-cycle  $A$ :

$$H = \frac{m}{nA}, \quad (30)$$

where the integers  $m, n$  correspond to the respective magnetic and electric charges;  $m$  is the quantized flux and  $n$  is the wrapping number of the higher dimensional brane around the corresponding internal 2-cycle. In the T-dual representation, associated to the inversion of the compactification radius along one of the two directions of the 2-cycle,  $m$  and  $n$  become the wrapping numbers around these two directions.

For simplicity, we consider first the case where the internal manifold is a product of three factorized tori  $\prod_{i=1}^3 T_{(i)}^2$ . Then, the mass formula (28) becomes:

$$\delta M^2 = \sum_i (2k_i + 1) |qH_i| + 2qH_i \Sigma_i, \quad (31)$$

where  $\Sigma_i$  is the projection of the internal helicity along the  $i$ -th plane. For a ten-dimensional (10d) spinor, its eigenvalues are  $\Sigma_i = \pm 1/2$ , while for a 10d vector  $\Sigma_i = \pm 1$  in one of the planes  $i = i_0$  and zero in the other two ( $i \neq i_0$ ). Thus, charged higher dimensional scalars become massive, fermions lead to chiral 4d zero modes if all  $H_i \neq 0$ , while the lightest scalars coming from 10d vectors have masses

$$M_0^2 = \begin{cases} |qH_1| + |qH_2| - |qH_3| \\ |qH_1| - |qH_2| + |qH_3| \\ -|qH_1| + |qH_2| + |qH_3| \end{cases}. \quad (32)$$

Note that all of them can be made positive definite, avoiding the Nielsen-Olesen instability, if all  $H_i \neq 0$ . Moreover, one can easily show that if a scalar mass vanishes, some supersymmetry remains unbroken [44, 45].

## 8 Minimal Standard Model embedding

We turn on now several abelian magnetic fields  $H_I^a$  of different Cartan generators  $U(1)_a$ , so that the gauge group is a product of unitary factors  $\prod_a U(N_a)$  with  $U(N_a) = SU(N_a) \times U(1)_a$ . In an appropriate T-dual representation, it amounts to consider several stacks of D6-branes intersecting in the three internal tori at angles. An open string with one end on the  $a$ -th stack has charge  $\pm 1$  under the  $U(1)_a$ , depending on its orientation, and is neutral with respect to all others.

In this section, we perform a general study of SM embedding in three brane stacks with gauge group  $U(3) \times U(2) \times U(1)$  [47], and present an explicit example having realistic particle content and satisfying gauge coupling unification [48]. We consider in general non oriented strings because of the presence of the orientifold plane that gives rise mirror branes with opposite magnetic fluxes  $m \rightarrow -m$  in eq. (30). An open string stretched between a brane stack  $U(N)$  and its mirror transforms in the symmetric or antisymmetric representation, while the multiplicity of chiral fermions is given by their intersection number.

The quark and lepton doublets ( $Q$  and  $L$ ) correspond to open strings stretched between the weak and the color or  $U(1)$  branes, respectively. On the other hand, the  $u^c$  and  $d^c$  antiquarks can come from strings that are either stretched between the color and  $U(1)$  branes, or that have both ends on the color branes (stretched between the brane stack and its orientifold image) and transform in the antisymmetric representation of  $U(3)$  (which is an anti-triplet). There are therefore three possible models, depending on whether it is the  $u^c$  (model A), or the  $d^c$  (model B), or none of them (model C), the state coming from the antisymmetric representation of color branes. It follows that the antilepton  $l^c$  comes in a similar way from open strings with both ends either on the weak brane stack and transforming in the antisymmetric representation of  $U(2)$  which is an  $SU(2)$  singlet (in model A), or on the abelian brane and transforming in the ‘‘symmetric’’ representation of  $U(1)$  (in models B and C). The three models are presented pictorially in Fig. 8

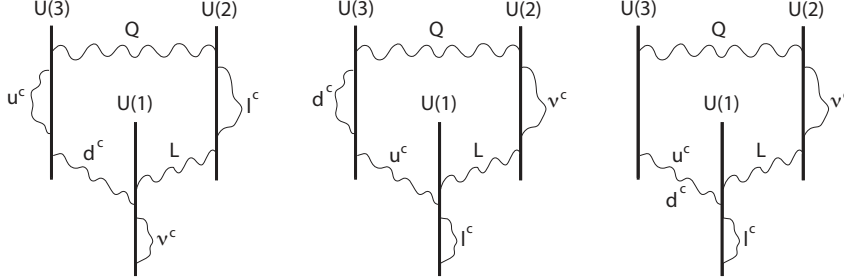


Figure 12: Pictorial representation of models A, B and C

Thus, the members of a family of quarks and leptons have the following quantum numbers:

	Model A	Model B	Model C
$Q$	$(\mathbf{3}, \mathbf{2}; 1, 1, 0)_{1/6}$	$(\mathbf{3}, \mathbf{2}; 1, \varepsilon_Q, 0)_{1/6}$	$(\mathbf{3}, \mathbf{2}; 1, \varepsilon_Q, 0)_{1/6}$
$u^c$	$(\bar{\mathbf{3}}, \mathbf{1}; 2, 0, 0)_{-2/3}$	$(\bar{\mathbf{3}}, \mathbf{1}; -1, 0, 1)_{-2/3}$	$(\bar{\mathbf{3}}, \mathbf{1}; -1, 0, 1)_{-2/3}$
$d^c$	$(\bar{\mathbf{3}}, \mathbf{1}; -1, 0, \varepsilon_d)_{1/3}$	$(\bar{\mathbf{3}}, \mathbf{1}; 2, 0, 0)_{1/3}$	$(\bar{\mathbf{3}}, \mathbf{1}; -1, 0, -1)_{1/3}$
$L$	$(\mathbf{1}, \mathbf{2}; 0, -1, \varepsilon_L)_{-1/2}$	$(\mathbf{1}, \mathbf{2}; 0, \varepsilon_L, 1)_{-1/2}$	$(\mathbf{1}, \mathbf{2}; 0, \varepsilon_L, 1)_{-1/2}$
$l^c$	$(\mathbf{1}, \mathbf{1}; 0, 2, 0)_1$	$(\mathbf{1}, \mathbf{1}; 0, 0, -2)_1$	$(\mathbf{1}, \mathbf{1}; 0, 0, -2)_1$
$\nu^c$	$(\mathbf{1}, \mathbf{1}; 0, 0, 2\varepsilon_\nu)_0$	$(\mathbf{1}, \mathbf{1}; 0, 2\varepsilon_\nu, 0)_0$	$(\mathbf{1}, \mathbf{1}; 0, 2\varepsilon_\nu, 0)_0$

where the last three digits after the semi-column in the brackets are the charges under the three abelian factors  $U(1)_3 \times U(1)_2 \times U(1)$ , that we will call  $Q_3$ ,  $Q_2$  and  $Q_1$  in the following, while the subscripts denote the corresponding hypercharges. The various sign ambiguities  $\varepsilon_i = \pm 1$  are due to the fact that the corresponding abelian factor does not participate in the hypercharge combination (see below). In the last lines, we also give the quantum numbers of a possible right-handed

neutrino in each of the three models. These are in fact all possible ways of embedding the SM spectrum in three sets of branes.

The hypercharge combination is:

$$\begin{aligned} \text{Model A} & : Y = -\frac{1}{3}Q_3 + \frac{1}{2}Q_2 \\ \text{Model B,C} & : Y = \frac{1}{6}Q_3 - \frac{1}{2}Q_1 \end{aligned} \quad (34)$$

leading to the following expressions for the weak angle:

$$\begin{aligned} \text{Model A} & : \sin^2 \theta_W = \frac{1}{2 + 2\alpha_2/3\alpha_3} = \frac{3}{8} \Big|_{\alpha_2=\alpha_3} \\ \text{Model B,C} & : \sin^2 \theta_W = \frac{1}{1 + \alpha_2/2\alpha_1 + \alpha_2/6\alpha_3} \\ & = \frac{6}{7 + 3\alpha_2/\alpha_1} \Big|_{\alpha_2=\alpha_3} \end{aligned} \quad (35)$$

In the second part of the above equalities, we used the unification relation  $\alpha_2 = \alpha_3$ , that can be imposed if for instance  $U(3)$  and  $U(2)$  branes are coincident, leading to a  $U(5)$  unified group. Alternatively, this condition can be generally imposed under mild assumptions [48]. It follows that model A admits natural gauge coupling unification of strong and weak interactions, and predicts the correct value for  $\sin^2 \theta_W = 3/8$  at the unification scale  $M_{\text{GUT}}$ . On the other hand, model B corresponds to the flipped  $SU(5)$  where the role of  $u^c$  and  $d^c$  is interchanged together with  $l^c$  and  $\nu^c$  between the  $\mathbf{10}$  and  $\bar{\mathbf{5}}$  representations [49].

Besides the hypercharge combination, there are two additional  $U(1)$ 's. It is easy to check that one of the two can be identified with  $B - L$ . For instance, in model A choosing the signs  $\varepsilon_d = \varepsilon_L = -\varepsilon_\nu = -\varepsilon_H = \varepsilon_{H'}$ , it is given by:

$$B - L = -\frac{1}{6}Q_3 + \frac{1}{2}Q_2 - \frac{\varepsilon_d}{2}Q_1. \quad (36)$$

Finally, the above spectrum can be easily implemented with a Higgs sector, since the Higgs field  $H$  has the same quantum numbers as the lepton doublet or its complex conjugate.

## 9 Moduli stabilization

Internal magnetic fluxes provide a new calculable method of moduli stabilization in four-dimensional (4d) type I string compactifications [50–52]. In fact, moduli stabilization in the presence of 3-form closed string fluxes led to significance progress over the last years [53, 54] but presents some drawbacks: (i) it has no exact string description and thus relies mainly on the low energy supergravity approximation; (ii) in the generic case, it can fix only the complex structure and the dilaton [55], while for the Kähler class non-perturbative effects have to be used [54]. On the other hand, constant internal magnetic fields

can stabilize mainly Kähler moduli [50, 56] and are thus complementary to 3-form closed string fluxes. Moreover, they can also be used in simple toroidal compactifications, stabilizing all geometric moduli in a supersymmetric vacuum using only magnetized  $D9$ -branes that have an exact perturbative string description [43, 57]. They have also a natural implementation in intersecting D-brane models.

Here, we make use of the conventions given in Appendix A of Ref. [51], for the parametrization of the torus  $T^6$ , as well as for the general definitions of the Kähler and complex structure moduli. In particular, the coordinates of three factorized tori:  $(T^2)^3 \in T^6$  are given by  $x_i, y_i$   $i = 1, 2, 3$  with periodicities:  $x^i = x^i + 1$ ,  $y^i \equiv y^i + 1$ , and a volume normalization:

$$\int dx_1 \wedge dy_1 \wedge dx_2 \wedge dy_2 \wedge dx_3 \wedge dy_3 = 1. \quad (37)$$

The 36 moduli of  $T^6$  correspond to 21 independent deformations of the internal metric and 15 deformations of the two-index antisymmetric tensor  $C_2$  from the RR closed string sector. They form nine complex parameters of Kähler class and nine of complex structure. Indeed, the geometric moduli decompose in a complex structure variation which is parametrized by the matrix  $\tau_{ij}$  entering in the definition of the complex coordinates

$$z_i = x_i + \tau_{ij} y^j, \quad (38)$$

and in the Kähler variation of the mixed part of the metric described by the real  $(1, 1)$ -form  $J = i\delta g_{i\bar{j}} dz^i \wedge d\bar{z}^{\bar{j}}$ . The later is complexified with the corresponding RR two-form deformation.

The stacks of  $D9$ -branes are characterized by three independent sets of data:

- (a) Their multiplicities  $N_a$ , that describe the rank of the the unitary gauge group  $U(N_a)$  on each  $D9$  stack.
- (b) The winding matrices  $W_{\hat{\alpha}}^{\hat{\alpha}, a}$  describing the covering of the world-volume of each stack- $a$  of  $D9$ -branes on the compactified ambient space. They are defined as  $W_{\hat{\alpha}}^{\hat{\alpha}} = \partial\xi^{\hat{\alpha}}/\partial X^{\alpha}$  for  $\alpha, \hat{\alpha} = 1, \dots, 6$ , where  $\xi^{\hat{\alpha}}$  and  $X^{\alpha}$  are the six internal coordinates on the world-volume and space-time, respectively. For simplicity, in the examples we consider here, the winding matrix  $W_{\hat{\alpha}}^{\hat{\alpha}}$  is chosen to be diagonal, implying that the world-volume and target space  $T^6$  coordinates are identified, up to a winding multiplicity factor  $n_{\hat{\alpha}}^a$  for each brane stack- $a$ :

$$n_{\hat{\alpha}}^a \equiv W_{\hat{\alpha}}^{\hat{\alpha}, a}. \quad (39)$$

- (c) The first Chern numbers  $m_{\hat{\alpha}\hat{\beta}}^a$  of the  $U(1)$  background on the branes world-volume. In other words, for each stack  $U(N_a) = U(1)_a \times SU(N_a)$ , the  $U(1)_a$  has a constant field strength on the covering of the internal space, which is a  $6 \times 6$  antisymmetric matrix. These are subject to the Dirac quantization condition which implies that all internal magnetic fluxes  $F_{\hat{\alpha}\hat{\beta}}^a$ , on the world-volume of each stack of  $D9$ -branes, are integrally quantized.

Explicitly, the world-volume fluxes  $F_{\hat{\alpha}\hat{\beta}}^a$  and the corresponding target space induced fluxes  $p_{\alpha\beta}^a$  are quantized as (see (30))

$$\begin{aligned} F_{\hat{\alpha}\hat{\beta}}^a &= m_{\hat{\alpha}\hat{\beta}}^a \in \mathbb{Z} \\ p_{\alpha\beta}^a &= (W^{-1})_{\hat{\alpha}}^{\hat{\alpha}, a} (W^{-1})_{\hat{\beta}}^{\hat{\beta}, a} m_{\hat{\alpha}\hat{\beta}}^a \in \mathbb{Q}. \end{aligned} \quad (40)$$

The complexified fluxes in the basis (38) can be written as

$$F_{(2,0)}^a = (\tau - \bar{\tau})^{-1T} [\tau^T p_{xx}^a \tau - \tau^T p_{xy}^a - p_{yx}^a \tau + p_{yy}^a] (\tau - \bar{\tau})^{-1} \quad (41)$$

$$F_{(1,1)}^a = (\tau - \bar{\tau})^{-1T} [-\tau^T p_{xx}^a \bar{\tau} + \tau^T p_{xy}^a + p_{yx}^a \bar{\tau} - p_{yy}^a] (\tau - \bar{\tau})^{-1} \quad (42)$$

where the matrices  $(p_{x^i x^j}^a)$ ,  $(p_{x^i y^j}^a)$  and  $(p_{y^i y^j}^a)$  are the quantized field strengths in target space, given in eq. (40). The field strengths  $F_{(2,0)}^a$  and  $F_{(1,1)}^a$  are  $3 \times 3$  matrices that correspond to the upper half of the matrix  $\mathcal{F}^a$ :

$$\mathcal{F}^a \equiv -(2\pi)^2 i \alpha' \begin{pmatrix} F_{(2,0)}^a & F_{(1,1)}^a \\ -F_{(1,1)}^{a\dagger} & F_{(2,0)}^{a*} \end{pmatrix}, \quad (43)$$

which is the total field strength in the cohomology basis  $e_{i\bar{j}} = idz^i \wedge d\bar{z}^j$ .

## 9.1 Supersymmetry conditions

The supersymmetry conditions then read [50, 51]:

$$1. \quad F_{(2,0)}^a = 0 \quad \forall a = 1, \dots, K, \quad (44)$$

for  $K$  brane stacks, stating that the purely holomorphic flux vanishes. For given flux quanta and winding numbers, this matrix equation restricts the complex structure  $\tau$ . Using eq. (41), it imposes a restriction on the parameters of the complex structure matrix elements  $\tau$ :

$$F_{(2,0)}^a = 0 \quad \rightarrow \quad \tau^T p_{xx}^a \tau - \tau^T p_{xy}^a - p_{yx}^a \tau + p_{yy}^a = 0, \quad (45)$$

giving rise to at most six complex equations for each brane stack  $a$ .

$$2. \quad \mathcal{F}_a \wedge \mathcal{F}_a \wedge \mathcal{F}_a = \mathcal{F}_a \wedge J \wedge J, \quad (46)$$

that gives rise to one real equation restricting the Kähler moduli. This can be understood as a D-flatness condition. In the 4d effective action, the magnetic fluxes give rise to topological couplings for the different axions of the compactified field theory. These arise from the dimensional reduction of the Wess Zumino action. In addition to the topological coupling, the  $\mathcal{N} = 1$  supersymmetric action yields a Fayet-Iliopoulos (FI) term of the form:

$$\frac{\xi_a}{g_a^2} = \frac{1}{(4\pi^2 \alpha')^3} \int_{T^6} (\mathcal{F}_a \wedge \mathcal{F}_a \wedge \mathcal{F}_a - \mathcal{F}_a \wedge J \wedge J). \quad (47)$$

The D-flatness condition in the absence of charged scalars requires then that  $\langle D_a \rangle = \xi_a = 0$ , which is equivalent to eq. (46). In the case where  $T^6$  is a product of three orthogonal 2-tori, this condition becomes

$$H_1 + H_2 + H_3 = H_1 H_2 H_3 \quad \Leftrightarrow \quad \theta_1 + \theta_2 + \theta_3 = 0, \quad (48)$$

in terms of the magnetic fields  $H_i$  along the internal planes defined in section 7, or equivalently in terms of the angles of D6-branes with respect to the orientifold axis.

$$3. \quad \det W_a (J \wedge J \wedge J - \mathcal{F}_a \wedge \mathcal{F}_a \wedge J) > 0, \quad (49)$$

which can also be understood from a 4d viewpoint as the positivity of the  $U(1)_a$  gauge coupling  $g_a^2$ . Indeed, its expression in terms of the fluxes and moduli reads

$$\frac{1}{g_a^2} = \frac{1}{(4\pi^2 \alpha')^3} \int_{T^6} (J \wedge J \wedge J - \mathcal{F}_a \wedge \mathcal{F}_a \wedge J). \quad (50)$$

In toroidal models with NS-NS vanishing  $B$ -field background, the net generation number of chiral fermions is in general even [58]. Thus, it is necessary to turn on a constant  $B$ -field in order to obtain a Standard Model like spectrum with three generations. Due to the world-sheet parity projection, the NS-NS two-index field  $B_{\alpha\beta}$  is projected out from the physical spectrum and constrained to take the discrete values 0 or  $1/2$  (in string units) along a 2-cycle  $(\alpha\beta)$  of  $T^6$  [59]. Its effect is simply accounted for by shifting the target space flux matrices  $p^a$  by  $p^a + B$  in all formulae.

The main ingredients for the moduli stabilization are [50, 51]:

- A set of nine magnetized  $D9$ -branes is needed to stabilize all 36 moduli of the torus  $T^6$  by the supersymmetry conditions [44, 60]. This follows from the second condition (46) above, in order to fix all nine Kähler class moduli. At the same time, all nine corresponding  $U(1)$  brane factors become massive by absorbing the RR partners of the Kähler moduli [44, 50]. This is due to a kinetic mixing between the  $U(1)$  gauge fields  $A^a$  and the RR axions, arising from the 10d Chern-Simons coupling involving the RR two-form  $C_2$  along its internal components:  $dC_2 \wedge \star(A^a \wedge \langle \mathcal{F}^a \rangle)$ .
- At least six of the magnetized brane stacks must have oblique fluxes given by mutually non-commuting matrices, in order to fix all off-diagonal components of the metric. The fluxes however can be chosen so that the metric is fixed in a diagonal form, as we will see below. At the same time, the complex structure RR moduli get stabilized by a potential generated through mixing with the metric moduli from the NS-NS (Neveu-Schwarz) closed string sector [52].
- The non-linear part of Dirac-Born-Infeld (DBI) action which is needed to fix the overall volume. This is only valid in 4d compactifications (and

Table 2: Six  $U(1)$  branes with oblique magnetic fluxes

Stack #	Fluxes	Fixed moduli	5-brane localization
#1 $N_1 = 1$	$(F_{x_1 y_2}^1, F_{x_2 y_1}^1) = (1, 1)$	$\tau_{31} = \tau_{32} = 0$ $\tau_{11} = \tau_{22}$ $\text{Re}J_{1\bar{2}} = 0$	$[x_3, y_3]$
#2 $N_2 = 1$	$(F_{x_1 y_3}^2, F_{x_3 y_1}^2) = (1, 1)$	$\tau_{21} = \tau_{23} = 0$ $\tau_{11} = \tau_{33}$ $\text{Re}J_{1\bar{3}} = 0$	$[x_2, y_2]$
#3 $N_3 = 1$	$(F_{x_1 x_2}^3, F_{y_1 y_2}^3) = (1, 1)$	$\tau_{13} = 0, \tau_{11}\tau_{22} = -1$ $\text{Im}J_{1\bar{2}} = 0$	$[x_3, y_3]$
#4 $N_4 = 1$	$(F_{x_2 x_3}^4, F_{y_2 y_3}^4) = (1, 1)$	$\tau_{12} = 0$ $\text{Im}J_{2\bar{3}} = 0$	$[x_1, y_1]$
#5 $N_5 = 1$	$(F_{x_1 x_3}^5, F_{y_1 y_3}^5) = (1, 1)$	$\text{Im}J_{1\bar{3}} = 0$	$[x_2, y_2]$
#6 $N_6 = 1$	$(F_{x_2 y_3}^6, F_{x_3 y_2}^6) = (1, 1)$	$\text{Re}J_{2\bar{3}} = 0$	$[x_1, y_1]$

not in higher dimensions). Indeed, in six dimensions, the condition (46) becomes  $\mathcal{F}^a \wedge J = 0$  which is homogeneous in  $J$  and thus cannot fix the internal volume.

Below, we give an explicit example of nine magnetized D-brane stacks stabilizing all  $T^6$  moduli in a way that the metric is fixed in a diagonal form [51]. The winding matrix  $W^a$  is chosen to be the identity, for simplicity. The first six  $U(1)$  branes with oblique fluxes are presented in Table 2. They fix all moduli except the areas of the three factorized 2-torii. These are fixed by adding three diagonal brane stacks displayed in the upper part of Table 3 (stacks #7, #8 and #9). These give the following restrictions on the diagonal Kähler moduli:

$$\begin{pmatrix} \mathcal{F}_1^7 & \mathcal{F}_2^7 & \mathcal{F}_3^7 \\ \mathcal{F}_1^8 & \mathcal{F}_2^8 & \mathcal{F}_3^8 \\ \mathcal{F}_1^9 & \mathcal{F}_2^9 & \mathcal{F}_3^9 \end{pmatrix} \begin{pmatrix} J_2 J_3 \\ J_1 J_3 \\ J_1 J_2 \end{pmatrix} = \begin{pmatrix} \mathcal{F}_1^7 \mathcal{F}_2^7 \mathcal{F}_3^7 \\ \mathcal{F}_1^8 \mathcal{F}_2^8 \mathcal{F}_3^8 \\ \mathcal{F}_1^9 \mathcal{F}_2^9 \mathcal{F}_3^9 \end{pmatrix}, \quad (51)$$

where the subscript  $i = 1, 2, 3$  denotes the diagonal element  $i\bar{i}$ . It follows that the moduli are fixed to the values:

$$\tau_{ij} = i\delta_{ij}; \quad J_{i\bar{j}} = 0; \quad (J_{x_1 y_1}, J_{x_2 y_2}, J_{x_3 y_3}) = 4\pi^2 \alpha' \sqrt{\frac{3}{22}}(44, 66, 19). \quad (52)$$

Table 3: Brane stacks with diagonal magnetic fluxes

Stack #	Multiplicity	Fluxes
#7	$N_7 = 1$	$(F_{x_1 y_1}^7, F_{x_2 y_2}^7, F_{x_3 y_3}^7) = (-4, -4, 3)$
#8	$N_8 = 2$	$(F_{x_1 y_1}^8, F_{x_2 y_2}^8, F_{x_3 y_3}^8) = (-3, 1, 1)$
#9	$N_9 = 3$	$(F_{x_1 y_1}^9, F_{x_2 y_2}^9, F_{x_3 y_3}^9) = (-2, 3, 0)$
#10	$N_{10} = 2$	$(F_{x_1 y_1}^{10}, F_{x_2 y_2}^{10}, F_{x_3 y_3}^{10}) = (5, 1, 2)$
#11	$N_{11} = 2$	$(F_{x_1 y_1}^{11}, F_{x_2 y_2}^{11}, F_{x_3 y_3}^{11}) = (0, 4, 1)$

Note that for every solution, an infinite discret family of vacua can be found in general by appropriate rescaling of fluxes and volumes. For instance, a uniform rescaling of all fluxes by the same (integer) factor  $\Lambda$  leads to new solutions where all areas  $J_i$  are rescaled by the same factor,  $J_i \rightarrow \Lambda J_i$ . These are large volume solutions that remain compatible with tadpole cancellation, as we will see below.

## 9.2 Tadpole cancellation conditions

In toroidal compactifications of type I string theory, the magnetized  $D9$ -branes induce 5-brane charges as well, while the 3-brane and 7-brane charges automatically vanish due to the presence of mirror branes with opposite flux. For general magnetic fluxes, RR tadpole conditions can be written in terms of the Chern numbers and winding matrix [51, 52] as:

$$16 = \sum_{a=1}^K N_a \det W_a \equiv \sum_{a=1}^K Q^{9,a}, \quad (53)$$

$$0 = \sum_{a=1}^K N_a \det W_a \epsilon^{\alpha\beta\delta\gamma\sigma\tau} p_{\delta\gamma}^a p_{\sigma\tau}^a \equiv \sum_{a=1}^K Q_{\alpha\beta}^{5,a}, \quad \forall \alpha, \beta = 1, \dots, 6. \quad (54)$$

The l.h.s. of eq. (53) arises from the contribution of the  $O9$ -plane. On the other hand, in toroidal compactifications there are no  $O5$ -planes and thus the l.h.s. of eq. (54) vanishes.

In the example presented above, all induced 5-brane tadpoles are diagonal despite the presence of oblique fluxes. Their localization is shown in the last column of Table 2. It turns out however that the conditions of supersymmetry and tadpole cancellation cannot be satisfied simultaneously in toroidal compactifications, as can also be seen in our example. Our strategy is therefore to add

extra branes in order to satisfy the RR tadpole conditions. These branes are not supersymmetric and generate a potential for the dilaton, which is the only remaining closed string modulus not fixed by the supersymmetry conditions of the first nine stacks, from the FI D-terms (47). One is then has two possibilities to obtain a consistent vacuum with stabilized moduli:

1. Keep supersymmetry by turning on VEVs for charged scalars on the extra brane stacks. In their presence, the D-flatness supersymmetry condition (46) gets modified and in the low energy approximation, it reads:

$$D_a = - \left( \sum_{\phi} q_a^{\phi} |\phi|^2 + M_s^2 \xi_a \right) = 0, \quad (55)$$

where  $\xi_a$  is given by eqs. (47) and (50). The sum is extended over all scalars  $\phi$  charged under the  $a$ -th  $U(1)_a$  with charge  $q_a^{\phi}$ . When one of these scalars acquire a non-vanishing VEV  $\langle |\phi| \rangle^2 = v_{\phi}^2$ , the condition (46) is modified to:

$$q_a v_a^2 \int_{T^6} (J \wedge J \wedge J - \mathcal{F}_a \wedge \mathcal{F}_a \wedge J) = M_s^2 \int_{T^6} (\mathcal{F}_a \wedge J \wedge J - \mathcal{F}_a \wedge \mathcal{F}_a \wedge \mathcal{F}_a). \quad (56)$$

Note that this is valid for small values of  $v_a$  (in string units), since the inclusion of charged scalars in the D-term is in principle valid only perturbatively.

Indeed, the model presented above can be implemented by two extra stacks #10 and #11 with diagonal fluxes, presented in the lower part of Table 3, so that all 9- and 5-brane RR tadpoles are cancelled [51]. These stacks can be made supersymmetric only in the presence of non-trivial VEV's for open string states charged under the corresponding  $U(1)$  gauge bosons. Let us then switch on VEV's for the fields  $\phi_{10}$  and  $\phi_{11}$ ,  $v_{10}$  and  $v_{11}$  respectively, transforming in the antisymmetric representations of the corresponding  $SU(2)$  gauge groups and charged under the  $U(1)$ 's of the last two stacks. From the quanta given in Table 3 and the values for the Kähler moduli (52), the positivity conditions (49) for these branes are satisfied. Moreover, since the Kähler form is already fixed, the supersymmetry conditions (56) determine the values of  $v_{10}$  and  $v_{11}$  as:

$$v_{10}^2 l_s^2 \simeq \frac{0.71}{q} \simeq 0.35 \quad ; \quad v_{11}^2 l_s^2 \simeq \frac{0.31}{q} \simeq 0.15, \quad (57)$$

where we used that the  $U(1)$  charge of the fields in the antisymmetric representation is  $q = 2$ . These VEV's break the two  $U(1)$  factors and the final gauge group of the model becomes  $SU(3) \times SU(2)^3$ . Finally, the above values of the VEV's are reasonably small in string units, consistently with our perturbative approach of including the charged scalar fields in the D-terms.

We have thus presented a model where the open string moduli corresponding to charged scalar VEV's are also fixed by the magnetic fluxes. In principle, the same method can be applied for stabilizing other open string moduli, as well. Note also that the discrete family of large volume solutions is still valid for fixed  $v_a$ . All of them have the same gauge symmetry but different couplings (50) and matter spectra.

2. Break supersymmetry by D-terms in a anti-de Sitter vacuum, by going “slightly” off-criticality and thus generating a tree-level bulk dilaton potential that can also fix the dilaton at weak string coupling [61]. If this breaking of supersymmetry arises on brane stacks independent from the Standard Model, its mediation involves gauge interactions and is of particular D-type. In particular, gauginos can acquire Dirac masses at one loop without breaking the R-symmetry, due to the extended supersymmetric nature of the gauge sector [62]. A more detail discussion is done in the next section.

### 9.3 Spectrum

For completeness, here we present the spectrum of magnetized branes in a toroidal background. The gauge sector of the spectrum follows from the open strings starting and ending on the same brane stack. The gauge symmetry group is given by a product of unitary groups  $\otimes_a U(N_a)$ , upon identification of the associated open strings attached on a given stack with the ones attached on its orientifold mirror. In addition to these vector bosons, the massless spectrum contains adjoint scalars and fermions forming  $\mathcal{N} = 4$ ,  $d = 4$  supermultiplets.

In the matter sector, the massless spectrum is obtained from the following open string states [44, 46]:

1. Open strings stretched between the  $a$ -th and  $b$ -th stack give rise to chiral spinors in the bifundamental representation  $(N_a, \bar{N}_b)$  of  $U(N_a) \times U(N_b)$ . Their multiplicity  $I_{ab}$  is given by [52]:

$$I_{ab} = \frac{\det W_a \det W_b}{(2\pi)^3} \int_{T^6} \left( q_a F_{(1,1)}^a + q_b F_{(1,1)}^b \right)^3, \quad (58)$$

where  $F_{(1,1)}^a$  (given in eqs. (42) and (43)) is the pullback of the integrally quantized world-volume flux  $m_{\hat{\alpha}\hat{\beta}}^a$  on the target torus in the complex basis (38), and  $q_a$  is the corresponding  $U(1)_a$  charge; in our case  $q_a = +1$  ( $-1$ ) for the fundamental (anti-fundamental representation).

For factorized toroidal compactifications  $T^6 = (T^2)^3$  with only diagonal fluxes  $p_{x^i y^i}$  ( $i = 1, 2, 3$ ), the multiplicities of chiral fermions, arising from strings starting from stack  $a$  and ending at  $b$  or vice versa, take the simple form

$$(N_a, \bar{N}_b) : I_{ab} = \prod_i (\hat{m}_i^a \hat{n}_i^b - \hat{n}_i^a \hat{m}_i^b),$$

$$(N_a, N_b) : I_{ab^*} = \prod_i (\hat{m}_i^a \hat{n}_i^b + \hat{n}_i^a \hat{m}_i^b). \quad (59)$$

where the integers  $\hat{m}_i^a, \hat{n}_i^a$  are defined by:

$$\hat{m}_i^a \equiv m_{x^i y^i}^a, \quad \hat{n}_1^a \equiv n_1^a n_2^a; \quad \hat{n}_2^a \equiv n_3^a n_4^a, \quad \hat{n}_3^a \equiv n_5^a n_6^a, \quad (60)$$

in terms of the magnetic fluxes  $m^a$  and winding numbers  $n^a$  of eqs. (40) and (39), respectively.

2. Open strings stretched between the  $a$ -th brane and its mirror  $a^*$  give rise to massless modes associated to  $I_{aa^*}$  chiral fermions. These transform either in the antisymmetric or symmetric representation of  $U(N_a)$ . For factorized toroidal compactifications  $(T^2)^3$ , the multiplicities of chiral fermions are given by;

$$\begin{aligned} \text{Antisymmetric : } & \frac{1}{2} \left( \prod_i 2\hat{m}_i^a \right) \left( \prod_j \hat{n}_j^a + 1 \right), \\ \text{Symmetric : } & \frac{1}{2} \left( \prod_i 2\hat{m}_i^a \right) \left( \prod_j \hat{n}_j^a - 1 \right). \end{aligned} \quad (61)$$

In generic configurations, where supersymmetry is broken by the magnetic fluxes, the scalar partners of the massless chiral spinors in twisted open string sectors (*i.e.* from non-trivial brane intersections) are massive (or tachyonic). Moreover, when a chiral index  $I_{ab}$  vanishes, the corresponding intersection of stacks  $a$  and  $b$  is non-chiral. The multiplicity of the non-chiral spectrum is then determined by extracting the vanishing factor and calculating the corresponding chiral index in higher dimensions.

#### 9.4 A supersymmetric $SU(5)$ GUT with stabilized moduli

A more realistic model of moduli stabilization with three generations of quarks and leptons can be obtained by realizing in the above framework the model A of section 8 with  $U(3)$  and  $U(2)$  coincident, giving rise to an  $SU(5)$  GUT [63]. To elaborate further, the model is described by twelve stacks of branes, namely  $U_5, U_1, O_1, \dots, O_8, A$ , and  $B$ , whose role is described below:

- The  $SU(5)$  gauge group arises from the open string states of stack- $U_5$  containing five magnetized branes. The remaining eleven stacks contain only a single magnetized brane. Also, the stack- $U_5$  containing the GUT gauge sector, contributes to the GUT particle spectrum through open string states which either start and end on itself (or on its orientifold image) or on the stack- $U_1$ , having only a single brane and therefore contributing an extra  $U(1)$ . More precisely, open strings stretched in the intersection of  $U(5)$  with its orientifold image give rise to 3 chiral generations in the

antisymmetric representation  $\mathbf{10}$  of  $SU(5)$ , while the intersection of  $U(5)$  with the orientifold image of  $U(1)$  gives 3 chiral states transforming as  $\bar{\mathbf{5}}$ . Finally, the intersection of  $U(5)$  with the  $U(1)$  is non chiral, giving rise to Higgs pairs  $\mathbf{5} + \bar{\mathbf{5}}$ . The magnetic fluxes along the various branes are constrained by the fact that the chiral fermion spectrum, mentioned above, of the  $SU(5)$  GUT should arise from these two sectors only.

- The eight single brane stacks  $O_1, \dots, O_8$ , contain oblique fluxes and generalize the set of the six stacks #1 - #6 of the previous toy model, in the presence of a  $B$ -field background needed to obtain odd number (three) of chiral fermions. A crucial property of these ‘oblique’ branes is that the combined induced 5-brane charge lies only along the three diagonal directions  $[x_i, y_i]$ .
- The eight ‘oblique’ branes together with  $U_5$  fix all geometric moduli by the supersymmetry conditions. The holomorphicity condition (44) stabilizes the complex structure moduli to the identity matrix, as in (52), while the D-flatness condition (46) for the nine stacks  $U_5, O_1, \dots, O_8$ , imposing the vanishing of the FI terms  $\xi_a$  (47), fix the nine Kähler moduli in a diagonal form. The residual diagonal 5-brane tadpoles of the branes in the stacks  $U_5, U_1, O_1, \dots, O_8$  are then cancelled by introducing the last two single brane stacks  $A$  and  $B$ , satisfying also the required 9-brane charge.
- The D-flatness conditions for the brane stacks  $U_1, A$  and  $B$  can also be satisfied, provided some VEVs of charged scalars living on these branes are turned on to cancel the corresponding FI parameters, according to eqs. (55) and (56). They all take values smaller than the string scale, consistently with their perturbative treatment, and break the three  $U(1)$  symmetries. On the other hand, the remaining nine  $U(1)$  brane factors become massive by absorbing the RR partners of the Kähler class moduli. As a result, all extra  $U(1)$ ’s are broken and the only leftover gauge symmetry is an  $SU(5)$  GUT. Furthermore, the intersections of the  $U(5)$  stack with any additional brane used for moduli stabilization are non-chiral, yielding the three families of quarks and leptons in the  $\mathbf{10} + \bar{\mathbf{5}}$  representations as the only chiral spectrum of the model (gauge non-singlet).

## 10 Gaugino masses and D-term gauge mediation

Here, we study the possibility of breaking supersymmetry by magnetic fluxes in a part of the theory, instead of turning on charged scalar VEVs, such as in the brane stacks #10 and #11 of the toy model of section 9.1, or in the stacks  $U_1, A$  and  $B$  of the  $SU(5)$  model discussed above. Since this breaking of supersymmetry is induced by D-terms, gaugino masses are vanishing at the tree-level, because they are protected by a (chiral) R-symmetry. This symmetry is broken in general in the presence of gravity by the gravitino mass, as well as by higher

order in  $\alpha'$  string corrections (on the branes). Both effects generate gaugino masses radiatively from a diagram involving at least one boundary, where the gauginos are localized, and having effective ‘genus’  $3/2$  [64].

For oriented strings, there are two possibilities: (1) one boundary and one handle, corresponding to one gravitational loop in the effective supergravity; (2) three boundaries, corresponding to two loops in the effective gauge theory. In the limit of small supersymmetry breaking compared to the string scale, both diagrams are reduced to topological amplitudes receiving contributions only from massless states:

- (1) The one loop gravitational contribution of the first diagram leads to gaugino masses  $m_{1/2}$  scaling as the third power of the gravitino mass  $m_{3/2}$ :

$$m_{1/2} \propto g_s^2 \frac{m_{3/2}^3}{M_s^2}. \quad (62)$$

On the other hand, scalars on the brane acquire generically one-loop mass corrections  $m_0$  from the annulus diagram [65]:  $m_0 \gtrsim g_s m_{3/2}^2 / M_s$ , implying that gaugino masses are suppressed relative to scalar masses:

$$m_{1/2}^2 \lesssim g_s \frac{m_0^3}{M_s}. \quad (63)$$

Fixing  $m_{1/2}$  in the TeV range, one then finds that scalars are much heavier  $m_0 \gtrsim 10^8$  GeV. Thus, this mechanism leads to a hierarchy between scalar and gaugino masses of the type required by split supersymmetry [66, 67].

- (2) Similarly, the gauge contribution of the second diagram leads to even larger hierarchy:

$$m_{1/2} \propto g_s^2 \frac{m_0^4}{M_s^3}, \quad (64)$$

with the proportionality constant given by the open string topological partition function  $F_{(0,3)}$  [68]. This result can be understood from the supersymmetric dimension seven chiral operator in the effective field theory:  $\int d^2\theta \mathcal{W}^2 \text{Tr} W^2$ , when the magnetized  $U(1)$  gauge superfield  $\mathcal{W}$  acquires an expectation value along its D-auxiliary component:  $\langle \mathcal{W} \rangle = \theta \langle D \rangle$  with  $\langle D \rangle \sim m_0^2$ . Thus, the gauginos appearing in the lowest component of the (non-abelian) gauge superfield  $W$  acquire the Majorana mass (64), which is in the TeV region when the scalar masses are of order  $10^{13} - 10^{14}$  GeV.

An alternative way to generate gaugino masses is by giving Dirac type masses. Indeed, in the toroidal models we studied above, we mentioned already that the gauge sector on the branes comes into multiplets of  $\mathcal{N} = 4$  extended supersymmetry and thus gauginos can be paired into Dirac massive fermions without breaking the R-symmetry [69]. This leads to the possibility of a new gauge mediation mechanism [70]. A prototype model can be studied with the following setup, based on two sets of magnetized brane stacks: the observable set  $\mathcal{O}$  and the hidden set  $\mathcal{H}$  [62, 69].

- The Standard Model gauge sector corresponds to open strings that propagate with both ends on the same stack of branes that belong to  $\mathcal{O}$ : it has therefore an extended  $\mathcal{N} = 4$  or  $\mathcal{N} = 2$  supersymmetry. Similarly, the ‘secluded’ gauge sector corresponds to strings with both ends on the hidden stack of branes  $\mathcal{H}$ .
- The Standard Model quarks and leptons come from open strings stretched between different stacks of branes in  $\mathcal{O}$  that intersect at fixed points of the internal six-torus  $T^6$  and have therefore  $\mathcal{N} = 1$  supersymmetry.
- The Higgs sector on the other hand corresponds to strings stretched between different stacks of branes in  $\mathcal{O}$  that intersect at fixed points of a  $T^4$  and are parallel along a  $T^2$ : it has therefore  $\mathcal{N} = 2$  supersymmetry and the two Higgs doublets form a hypermultiplet. Finally, the messenger sector contains strings stretched between stacks of branes in  $\mathcal{O}$  and the hidden branes  $\mathcal{H}$ , that form also  $\mathcal{N} = 2$  hypermultiplets. Moreover, the two stacks of branes along the  $T^2$  are separated by a distance  $1/M$ , which introduces a supersymmetric mass  $M$  to the hypermultiplet messengers. The latter are also charged under the magnetized  $U(1)$ (s) that break supersymmetry in the ‘secluded’ sector  $\mathcal{H}$  via D-terms.

The main properties of this mechanism are:

1. The gauginos obtain Dirac masses at one loop given by:

$$m_{1/2}^D \sim \frac{\alpha}{4\pi} \frac{D}{M}, \quad (65)$$

where  $\alpha$  is the corresponding gauge coupling constant.

2. Scalar quarks and leptons acquire masses by one-loop diagrams involving Dirac gauginos in the effective theory where messengers have been integrated out (three-loop diagrams in the underlying theory). Their contributions are finite and one-loop suppressed with respect to gaugino masses [71, 72].
3. The tree-level Higgs potential gets modified because of its  $\mathcal{N} = 2$  structure.

$$V = V_{\text{soft}} + \frac{1}{8}(g^2 + g'^2)(|H_1|^2 - |H_2|^2)^2 + \frac{1}{2}(g^2 + g'^2)|H_1 H_2|^2, \quad (66)$$

where  $H_{1,2}$  are the two Higgs doublets,  $g$  and  $g'$  are the  $SU(2)$  and  $U(1)$  couplings, and the last term is a genuine  $\mathcal{N} = 2$  contribution which is absent in the MSSM. It follows that the lightest Higgs behaves as in the (non supersymmetric) Standard Model with no  $\tan\beta$  dependence on its couplings to fermions. On the other hand, the heaviest Higgs plays no role in electroweak symmetry breaking and does not couple to the  $Z$ -boson. In fact, the model behaves as the MSSM at large  $\tan\beta$  and the ‘little’ fine-tuning problem is significantly reduced [62].

4. The supersymmetric flavor problem is solved as in usual gauge mediation. Moreover, there is a common supersymmetry breaking scale in the observable sector, the masses of all supersymmetric particles being proportional to powers of gauge couplings. Finally, there are distinct collider signals different from that of the MSSM.

In conclusion, the framework of toroidal string compactifications with magnetized branes described above, starting from section 7, offers an interesting self-consistent setup for string phenomenology, in which one can build simple calculable models of particle physics with stabilized moduli and implement low energy supersymmetry breaking that can be studied directly at the string level.

## Acknowledgments

This work was supported in part by the European Commission under the RTN contract MRTN-CT-2004-503369, and in part by the INTAS contract 03-51-6346.

## References

- [1] For a review, see e.g. K. R. Dienes, *Phys. Rept.* **287** (1997) 447 [arXiv:hep-th/9602045]; and references therein.
- [2] C. Angelantonj and A. Sagnotti, *Phys. Rept.* **371** (2002) 1 [Erratum-ibid. **376** (2003) 339] [arXiv:hep-th/0204089].
- [3] I. Antoniadis, *Phys. Lett. B* **246** (1990) 377.
- [4] D. J. Kapner, T. S. Cook, E. G. Adelberger, J. H. Gundlach, B. R. Heckel, C. D. Hoyle and H. E. Swanson, *Phys. Rev. Lett.* **98** (2007) 021101.
- [5] N. Arkani-Hamed, S. Dimopoulos and G. R. Dvali, *Phys. Lett. B* **429** (1998) 263 [arXiv:hep-ph/9803315]; I. Antoniadis, N. Arkani-Hamed, S. Dimopoulos and G. R. Dvali, *Phys. Lett. B* **436** (1998) 257 [arXiv:hep-ph/9804398].
- [6] For a review see e.g. I. Antoniadis, *Prepared for NATO Advanced Study Institute and EC Summer School on Progress in String, Field and Particle Theory, Cargese, Corsica, France (2002)*; and references therein.
- [7] J. D. Lykken, *Phys. Rev. D* **54** (1996) 3693 [arXiv:hep-th/9603133].
- [8] J. C. Long and J. C. Price, *Comptes Rendus Physique* **4** (2003) 337; R. S. Decca, D. Lopez, H. B. Chan, E. Fischbach, D. E. Krause and C. R. Jamell, *Phys. Rev. Lett.* **94** (2005) 240401; R. S. Decca et al., arXiv:0706.3283 [hep-ph]; S. J. Smullin, A. A. Geraci, D. M. Weld, J. Chiverini, S. Holmes and A. Kapitulnik, arXiv:hep-ph/0508204; H. Abele, S. Haeßler and A. Westphal, in 271th WE-Heraeus-Seminar, Bad Honnef (2002).

- [9] I. Antoniadis and K. Benakli, *Phys. Lett. B* **326** (1994) 69.
- [10] K. R. Dienes, E. Dudas and T. Gherghetta, *Phys. Lett. B* **436** (1998) 55 [arXiv:hep-ph/9803466]; *Nucl. Phys. B* **537** (1999) 47 [arXiv:hep-ph/9806292].
- [11] I. Antoniadis, K. Benakli and M. Quirós, *Phys. Lett. B* **331** (1994) 313 and *Phys. Lett. B* **460** (1999) 176; P. Nath, Y. Yamada and M. Yamaguchi, *Phys. Lett. B* **466** (1999) 100 T. G. Rizzo and J. D. Wells, *Phys. Rev. D* **61** (2000) 016007; T. G. Rizzo, *Phys. Rev. D* **61** (2000) 055005; A. De Rujula, A. Donini, M. B. Gavela and S. Rigolin, *Phys. Lett. B* **482** (2000) 195;
- [12] E. Accomando, I. Antoniadis and K. Benakli, *Nucl. Phys. B* **579** (2000) 3.
- [13] I. Antoniadis, K. Benakli and A. Laugier, *JHEP* **0105** (2001) 044.
- [14] P. Nath and M. Yamaguchi, *Phys. Rev. D* **60** (1999) 116004; *Phys. Rev. D* **60** (1999) 116006; M. Masip and A. Pomarol, *Phys. Rev. D* **60** (1999) 096005; W. J. Marciano, *Phys. Rev. D* **60** (1999) 093006; A. Strumia, *Phys. Lett. B* **466** (1999) 107; R. Casalbuoni, S. De Curtis, D. Dominici and R. Gatto, *Phys. Lett. B* **462** (1999) 48; C. D. Carone, *Phys. Rev. D* **61** (2000) 015008; A. Delgado, A. Pomarol and M. Quirós, *JHEP* **1** (2000) 30.
- [15] G. Servant and T. M. P. Tait, *Nucl. Phys. B* **650** (2003) 391.
- [16] G. F. Giudice, R. Rattazzi and J. D. Wells, *Nucl. Phys. B* **544** (1999) 3; E. A. Mirabelli, M. Perelstein and M. E. Peskin, *Phys. Rev. Lett.* **82** (1999) 2236; T. Han, J. D. Lykken and R. Zhang, *Phys. Rev. D* **59** (1999) 105006; K. Cheung and W.-Y. Keung, *Phys. Rev. D* **60** (1999) 112003; C. Balázs *et al.*, *Phys. Rev. Lett.* **83** (1999) 2112; L3 Collaboration (M. Acciarri *et al.*), *Phys. Lett. B* **464** (1999) 135 and **470** (1999) 281; J. L. Hewett, *Phys. Rev. Lett.* **82** (1999) 4765.
- [17] N. Arkani-Hamed, S. Dimopoulos and G. Dvali, *Phys. Rev. D* **59** (1999) 086004.
- [18] S. Cullen and M. Perelstein, *Phys. Rev. Lett.* **83** (1999) 268; V. Barger, T. Han, C. Kao and R. J. Zhang, *Phys. Lett. B* **461** (1999) 34.
- [19] K. Benakli and S. Davidson, *Phys. Rev. D* **60** (1999) 025004; L. J. Hall and D. Smith, *Phys. Rev. D* **60** (1999) 085008.
- [20] E. Dudas and J. Mourad, *Nucl. Phys. B* **575** (2000) 3 [arXiv:hep-th/9911019]; S. Cullen, M. Perelstein and M. E. Peskin, *Phys. Rev. D* **62** (2000) 055012; D. Bourilkov, *Phys. Rev. D* **62** (2000) 076005; L3 Collaboration (M. Acciarri *et al.*), *Phys. Lett. B* **489** (2000) 81.
- [21] P. C. Argyres, S. Dimopoulos and J. March-Russell, *Phys. Lett. B* **441** (1998) 96 [arXiv:hep-th/9808138]; T. Banks and W. Fischler, arXiv:hep-th/9906038.

- [22] S. B. Giddings and S. Thomas, *Phys. Rev. D* **65** (2002) 056010 [arXiv:hep-ph/0106219]; S. Dimopoulos and G. Landsberg, *Phys. Rev. Lett.* **87** (2001) 161602 [arXiv:hep-ph/0106295].
- [23] P. Meade and L. Randall, arXiv:0708.3017 [hep-ph].
- [24] I. Antoniadis, C. Bachas, *Phys. Lett. B* **450** (1999) 83.
- [25] I. Antoniadis, K. Benakli, A. Laugier and T. Maillard, *Nucl. Phys. B* **662** (2003) 40 [arXiv:hep-ph/0211409].
- [26] I. Antoniadis, S. Dimopoulos and G. Dvali, *Nucl. Phys. B* **516** (1998) 70; S. Ferrara, C. Kounnas and F. Zwirner, *Nucl. Phys. B* **429** (1994) 589.
- [27] E. G. Adelberger, B. R. Heckel, S. Hoedl, C. D. Hoyle, D. J. Kapner and A. Upadhye, *Phys. Rev. Lett.* **98** (2007) 131104.
- [28] T. R. Taylor and G. Veneziano, *Phys. Lett. B* **213** (1988) 450.
- [29] I. Antoniadis, E. Kiritsis and J. Rizos, *Nucl. Phys. B* **637** (2002) 92.
- [30] E. Dudas and J. Mourad, *Phys. Lett. B* **514** (2001) 173 [arXiv:hep-th/0012071].
- [31] D. V. Volkov and V. P. Akulov, *JETP Lett.* **16** (1972) 438 and *Phys. Lett. B* **46** (1973) 109.
- [32] A. Brignole, F. Feruglio and F. Zwirner, *JHEP* **9711** (1997) 001; T. E. Clark, T. Lee, S. T. Love and G. Wu, *Phys. Rev. D* **57** (1998) 5912; M. A. Luty and E. Ponton, *Phys. Rev. D* **57** (1998) 4167; I. Antoniadis, K. Benakli and A. Laugier, *Nucl. Phys. B* **631** (2002) 3.
- [33] I. Antoniadis and M. Tuckmantel, *Nucl. Phys. B* **697** (2004) 3.
- [34] I. Antoniadis, M. Tuckmantel and F. Zwirner, *Nucl. Phys. B* **707** (2005) 215 [arXiv:hep-ph/0410165].
- [35] I. Antoniadis, K. Benakli and M. Quirós, *Nucl. Phys. B* **583** (2000) 35.
- [36] I. Antoniadis, K. Benakli and M. Quiros, *New Jour. Phys.* **3** (2001) 20.
- [37] I. Antoniadis, C. Muñoz and M. Quirós, *Nucl. Phys. B* **397** (1993) 515; I. Antoniadis and M. Quirós, *Phys. Lett. B* **392** (1997) 61; A. Pomarol and M. Quirós, *Phys. Lett. B* **438** (1998) 225; I. Antoniadis, S. Dimopoulos, A. Pomarol and M. Quirós, *Nucl. Phys. B* **544** (1999) 503; A. Delgado, A. Pomarol and M. Quirós, *Phys. Rev. D* **60** (1999) 095008; R. Barbieri, L. J. Hall and Y. Nomura, *Phys. Rev. D* **63** (2001) 105007.
- [38] I. Antoniadis, E. Kiritsis and T. N. Tomaras, *Phys. Lett. B* **486** (2000) 186; I. Antoniadis, E. Kiritsis, J. Rizos and T. N. Tomaras, *Nucl. Phys. B* **660** (2003) 81.

- [39] G. Shiu and S.-H. H. Tye, *Phys. Rev. D* **58** (1998) 106007; Z. Kakushadze and S.-H. H. Tye, *Nucl. Phys. B* **548** (1999) 180; L. E. Ibáñez, C. Muñoz and S. Rigolin, *Nucl. Phys. B* **553** (1999) 43.
- [40] K. R. Dienes, E. Dudas and T. Gherghetta, *Nucl. Phys. B* **557** (1999) 25 [arXiv:hep-ph/9811428]; N. Arkani-Hamed, S. Dimopoulos, G. R. Dvali and J. March-Russell, *Phys. Rev. D* **65** (2002) 024032 [arXiv:hep-ph/9811448]; G. R. Dvali and A. Y. Smirnov, *Nucl. Phys. B* **563** (1999) 63.
- [41] A. Sagnotti, *Phys. Lett. B* **294** (1992) 196; L. E. Ibáñez, R. Rabadán and A. M. Uranga, *Nucl. Phys. B* **542** (1999) 112; E. Poppitz, *Nucl. Phys. B* **542** (1999) 31.
- [42] H. Davoudiasl, P. Langacker and M. Perelstein, *Phys. Rev. D* **65** (2002) 105015 [arXiv:hep-ph/0201128].
- [43] C. Bachas, arXiv:hep-th/9503030.
- [44] C. Angelantonj, I. Antoniadis, E. Dudas and A. Sagnotti, *Phys. Lett. B* **489** (2000) 223 [arXiv:hep-th/0007090].
- [45] M. Berkooz, M. R. Douglas and R. G. Leigh, *Nucl. Phys. B* **480** (1996) 265 [arXiv:hep-th/9606139].
- [46] R. Blumenhagen, L. Goerlich, B. Kors and D. Lust, *JHEP* **0010** (2000) 006 [arXiv:hep-th/0007024]; G. Aldazabal, S. Franco, L. E. Ibanez, R. Rabadan and A. M. Uranga, *J. Math. Phys.* **42** (2001) 3103 [arXiv:hep-th/0011073]; N. Ohta and P. K. Townsend, *Phys. Lett. B* **418** (1998) 77 [arXiv:hep-th/9710129].
- [47] I. Antoniadis, E. Kiritsis and T. N. Tomaras, *Phys. Lett. B* **486** (2000) 186 [arXiv:hep-ph/0004214]; I. Antoniadis, E. Kiritsis, J. Rizos and T. N. Tomaras, *Nucl. Phys. B* **660** (2003) 81 [arXiv:hep-th/0210263]; R. Blumenhagen, B. Kors, D. Lust and T. Ott, *Nucl. Phys. B* **616** (2001) 3 [arXiv:hep-th/0107138]; M. Cvetič, G. Shiu and A. M. Uranga, *Nucl. Phys. B* **615**, 3 (2001) [arXiv:hep-th/0107166]; I. Antoniadis and J. Rizos, 2003 unpublished work.
- [48] I. Antoniadis and S. Dimopoulos, *Nucl. Phys. B* **715**, 120 (2005) [arXiv:hep-th/0411032].
- [49] S. M. Barr, *Phys. Lett. B* **112** (1982) 219; J. P. Derendinger, J. E. Kim and D. V. Nanopoulos, *Phys. Lett. B* **139** (1984) 170; I. Antoniadis, J. R. Ellis, J. S. Hagelin and D. V. Nanopoulos, *Phys. Lett. B* **194** (1987) 231.
- [50] I. Antoniadis and T. Maillard, *Nucl. Phys. B* **716** (2005) 3, [arXiv:hep-th/0412008].
- [51] I. Antoniadis, A. Kumar, T. Maillard, arXiv: hep-th/0505260; *Nucl. Phys. B* **767** (2007) 139, [arXiv:hep-th/0610246].

- [52] M. Bianchi and E. Trevigne, JHEP **0508** (2005) 034, [arXiv:hep-th/0502147] and JHEP **0601** (2006) 092, [arXiv:hep-th/0506080].
- [53] S. B. Giddings, S. Kachru and J. Polchinski, Phys. Rev. D **66** (1997) 106006, [arXiv:hep-th/0105097].
- [54] R. Kallosh, S. Kachru, A. Linde and S. Trivedi, Phys. Rev. D **68** (2003) 046005, [arXiv:hep-th/0301240].
- [55] S. Kachru, M.B. Schulz and S. Trivedi, JHEP **0310** (2003) 007, [arXiv:hep-th/0201028]; A. Frey and J. Polchinski, Phys. Rev. D **65** (2002) 126009, [arXiv:hep-th/0201029].
- [56] R. Blumenhagen, D. Lust and T. R. Taylor, Nucl. Phys. B **663** (2003) 319 [arXiv:hep-th/0303016]; J. F. G. Cascales and A. M. Uranga, JHEP **0305** (2003) 011 [arXiv:hep-th/0303024].
- [57] E. S. Fradkin and A. A. Tseytlin, Phys. Lett. B **163** (1985) 123; A. Abouelsaood, C. G. Callan, C. R. Nappi and S. A. Yost, Nucl. Phys. B **280** (1987) 599;
- [58] R. Blumenhagen, B. Kors and D. Lust, JHEP **0102** (2001) 030 [arXiv:hep-th/0012156].
- [59] M. Bianchi, G. Pradisi and A. Sagnotti, Nucl. Phys. B **376** (1992) 365; C. Angelantonj, Nucl. Phys. B **566** (2000) 126 [arXiv:hep-th/9908064]; C. Angelantonj and A. Sagnotti, arXiv:hep-th/0010279;
- [60] M. Marino, R. Minasian, G. W. Moore and A. Strominger, JHEP **0001** (2000) 005, [arXiv:hep-th/9911206].
- [61] I. Antoniadis, J.-P. Derendinger and T. Maillard, to appear.
- [62] I. Antoniadis, K. Benakli, A. Delgado, M. Quiros and M. Tuckmantel, Nucl. Phys. B **744** (2006) 156 [arXiv:hep-th/0601003]; I. Antoniadis, K. Benakli, A. Delgado and M. Quiros, arXiv:hep-ph/0610265.
- [63] I. Antoniadis, A. Kumar and B. Panda, arXiv:0709.2799 [hep-th].
- [64] I. Antoniadis and T. R. Taylor, Nucl. Phys. B **695** (2004) 103 [arXiv:hep-th/0403293] and Nucl. Phys. B **731** (2005) 164 [arXiv:hep-th/0509048].
- [65] I. Antoniadis, E. Dudas and A. Sagnotti, Nucl. Phys. B **544** (1999) 469 [arXiv:hep-th/9807011].
- [66] N. Arkani-Hamed and S. Dimopoulos, JHEP **0506** (2005) 073 [arXiv:hep-th/0405159]; G. F. Giudice and A. Romanino, Nucl. Phys. B **699** (2004) 65 [Erratum-ibid. B **706** (2005) 65] [arXiv:hep-ph/0406088].

- [67] I. Antoniadis and S. Dimopoulos, Nucl. Phys. B **715** (2005) 120 [arXiv:hep-th/0411032].
- [68] I. Antoniadis, K. S. Narain and T. R. Taylor, Nucl. Phys. B **729** (2005) 235 [arXiv:hep-th/0507244].
- [69] I. Antoniadis, A. Delgado, K. Benakli, M. Quiros and M. Tuckmantel, Phys. Lett. B **634** (2006) 302 [arXiv:hep-ph/0507192] and Nucl. Phys. B **744** (2006) 156 [arXiv:hep-th/0601003].
- [70] I. Antoniadis, K. Benakli, A. Delgado and M. Quiros, arXiv:hep-ph/0610265.
- [71] I. Antoniadis and K. Benakli, Phys. Lett. B **295** (1992) 219 [Erratum-ibid. B **407** (1997) 449] [arXiv:hep-th/9209020].
- [72] P. J. Fox, A. E. Nelson and N. Weiner, JHEP **0208** (2002) 035 [arXiv:hep-ph/0206096].